12-2018

New CA-ID-TIMS Detrital Zircon Constraints on Middle Neoproterozoic Sedimentary Successions, Southwestern United States

Abigail R. Bullard
Utah State University

NEW CA-ID-TIMS DETRITAL ZIRCON CONSTRAINTS ON MIDDLE NEOPROTEROZOIC SEDIMENTARY SUCCESSIONS, SOUTHWESTERN UNITED STATES

by

Abigail R. Bullard

A thesis submitted in partial fulfillment
of the requirements for the degree

of

MASTER OF SCIENCE

in

Geology

Approved:

_____	_____
Carol M. Dehler, Ph.D. Major Professor	Joel L. Pederson, Ph.D. Committee Member
_____	_____
John W. Shervais, Ph.D. Committee Member	Laurens H. Smith, Ph.D. Interim Vice President for Research and Dean of the School of Graduate Studies

UTAH STATE UNIVERSITY
Logan, Utah

2018

A B S T R A C T

New CA-ID-TIMS U-Pb detrital zircon constraints on middle Neoproterozoic sedimentary successions, southwestern U.S.

by

Abigail R. Bullard, Master of Science

Utah State University, 2018

Major Professor: Dr. Carol Dehler
Department: Geology

The correlative Neoproterozoic Chuar Group (Grand Canyon, AZ), Uinta Mountain Group (northeastern UT), and (middle) Pahrump Group (Death Valley, CA), together referred to as ChUMP, record deposition in intracratonic basins during the nascent rifting of Rodinia. Despite being some of the most thoroughly dated Neoproterozoic successions in the world previous detrital zircon U-Pb maximum depositional ages for the ChUMP units possess errors in excess of 1%, limiting efforts to constrain the timing of late Tonian Earth system evolution.

We report improved U-Pb maximum age constraints on these units obtained by subjecting detrital zircon grains previously dated by laser ablation methods to high-precision, chemical abrasion isotope-dilution thermal-ionization-mass-spectrometry (CA-ID-TIMS) analysis. These new data significantly improve the precision of ChUMP maximum depositional ages, with a mean age of 775.63 ± 0.27

Ma acquired for the base of the Nankoweap formation (Chuar Group), where previous work puts the age at 782 Ma. A mean age of 775.44 ± 0.73 Ma for the Horse Thief Springs formation (Pahrump Group) is also younger than the previously reported 787 ± 11 Ma. Zircons of the Moosehorn Lake and Outlaw Trail formations of the Uinta Mountain Group provide individual ages of about 766.88 ± 2.31 Ma, which is consistent with a previously reported age of 766.4 ± 4.8 Ma. These high precision ages for the young detrital zircons in the ChUMP units improve correlations and provide better context for geochemical, isotopic, and biotic events that occurred during the initial rifting of Rodinia.

(69 pages)

PUBLIC ABSTRACT

New CA-ID-TIMS U-Pb detrital zircon constraints on middle Neoproterozoic sedimentary successions, southwestern U.S.

Abigail R. Bullard

Three related sedimentary successions located in Arizona, Utah, and California were deposited in basins on proto-North America during the early rifting of Rodinia (~780 Mya). Previous detrital zircon U-Pb maximum ages for the units are inexact, making it difficult to piece together what happened at this point in Earth history.

We report better maximum age constraints on these units obtained by subjecting detrital zircons to high-precision CA-ID-TIMS analysis, which provide more exact $^{206}Pb/^{238}U$ ages. These new data significantly improve the precision for the base of the ChUMP units, with an average age of 775.63 ± 0.27 Ma acquired for the bottom of the Chuar Group, where earlier work put the age at 782 Ma. An average age of 775.44 ± 0.73 Ma for the bottom of the Pahrump Group is also younger than the previously reported 787 ± 11 Ma. Zircons of the Uinta Mountain Group provided ages of about 766.88 ± 2.31 Ma, which is on par with an earlier age of 766.4 ± 4.8 Ma. These high precision ages for the young detrital zircons in the ChUMP units improve links between the units and provide better context for geochemical, isotopic, and biological events that occurred during the initial rifting of Rodinia.

ACKNOWLEDGMENTS

I would like to thank Dr. Carol Dehler for taking me under her tutelage; Dr. Mark Schmitz for the access he provided to his lab as well as many hours of training and instruction; my committee members Drs. Joel Pederson and John Shervis for their assistance in helping me see this through; and Drs. Jim Evans and Alexis Ault, for their service as committee members previously and their input on setting me on my eventual path. This research would have never come to fruition without the involvement of each and every one of you, and for that I am sincerely grateful.

I would like to extend a very special thanks to the Utah State University Geology Department, the Geological Society of America, and Mount Zion United Church of Christ, for providing me with the resources to see this project to completion.

Special thanks goes to my family, who have stood by me even when distance prevented them from doing so in the flesh. Thanks also goes to my friends and colleagues who have endured many a crisis as well as celebrated many a success with me. I never would have made it here without you.

Abigail R. Bullard

CONTENTS

Page

LIST OF TABLES

LIST OF FIGURES

INTRODUCTION

U-Pb detrital zircon geochronology has been revolutionary in constraining the maximum depositional ages of siliciclastic successions that otherwise lack dateable material or effective index fossils, particularly those of Precambrian time. The middle Neoproterozoic Chuar, Uinta Mountain, and Pahrump (ChUMP) group successions of SW Laurentia are a success story in this respect. Constrained by U-Pb geochronology, they are some of the best dated middle Neoproterozoic sedimentary successions in the world. However, detrital zircon U-Pb maximum depositional ages for the ChUMP units possess errors in excess of 1% (Dehler et al. 2010, Mahon et al. 2014, Dehler et al., 2017), saddling these maximum ages with, at times, tens of millions of years of uncertainty. This limits efforts to constrain the timing of late Tonian Earth system evolution.

The large body of geochronological data already in existence for the ChUMP groups reflects the fascination with these units within the geosciences and, to some degree, their amenability to geochronologic studies, despite their near lack of tuffaceous material. These rocks document intracratonic basin formation related to the rifting of the supercontinent Rodinia (Timmons et al., 2001; Dehler et al. 2010, Li et al., 2013; Mahon et al. 2014; Cox et al., 2016); contain abundant microfossils that exhibit diversity and complexity of life rarely chronicled in Neoproterozoic rocks (Ford and Breed, 1973; Horodyski, 1993; Porter and Knoll, 2000; Dehler et al., 2007; Dehler, 2014; Porter, 2016; Porter and Riedman, 2016); record meter-scale facies repetitions exhibiting Milankovitch cyclicity (Dehler et al., 2001), and record large-scale variability in C-isotope values attributed to varying rates of long-term carbon

burial across Laurentia (Dehler et al., 2017). These sedimentary archives can be of even greater value with precise geochronology to constrain the timing and duration of these events.

Here we report the acquisition of higher precision ages from new and previously identified detrital zircon populations of "ChUMP" basal formations using chemical abrasion-isotope dissolution-thermal ionization mass spectrometry (CA-ID-TIMS). These highly precise ages condense the currently recognized duration for the deposition of these strata by millions of years. CA-ID-TIMS provides higher precision data than laser ablation inductively coupled plasma mass spectrometry (LA-ICP-MS), because it removes zircon domains that have lost Pb and analyzes the residual, closed-system zircon. This removes many of the sources of error usually inherent in analyzing the isotopic ages of zircons (Mattinson, 2005).

GEOLOGIC BACKGROUND

Middle Neoproterozoic Successions of the Southwestern United States

Chuar Group, Grand Canyon Arizona

The well preserved and unmetamorphosed Chuar Group (1700 m thick) comprises variegated, organic-rich shale, with some thin but recurring sandstone and carbonate beds (Ford and Breed, 1973; Dehler et al., 2001; Dehler et al., 2017). It is only exposed in tributaries of the Colorado River in the eastern part of the Grand Canyon, covering an area of ca. 150 km^2 (**Fig. 1**).

The lowermost unit of the Chuar Group, and a focus of this study, is the Nankoweap Formation (Van Gundy, 1951; Dehler et al., 2017). Bracketed above and beneath by unconformities, it is a 120 meter thick section of red mudstone and red-to-white quartz arenite (**Fig.2**) (Timmons et al., 2001).

Chuar deposition likely occurred in an intracratonic extensional basin (Sears, 1990; Timmons et al., 2001; Dehler et al., 2001). The Chuar syncline and related Butte Fault, which trend N-S, are the primary structures related to the Chuar Group and were intermittently active during deposition (Timmons et al., 2001). Paleomagnetic work places the Chuar Group at ~15° S during Nankoweap time, 2° S latitude during Galeros time, and 18° N latitude during Kwagunt time (Weil et al., 2003; 2004). This and other work by Weil (2003, 2006) suggest that Rodinia was breaking up by 750 Ma, coinciding with Chuar Group deposition (Karlstrom et al., 2000; Dehler et al., 2017).

Fig. 1: Location map of the ChUMP units. Red is the location of the Chuar Group, Grand Canyon; blue is the mapped extent of the Uinta Mountain Group, NE Utah; and green is the location of the Pahrump Group, Death Valley California.

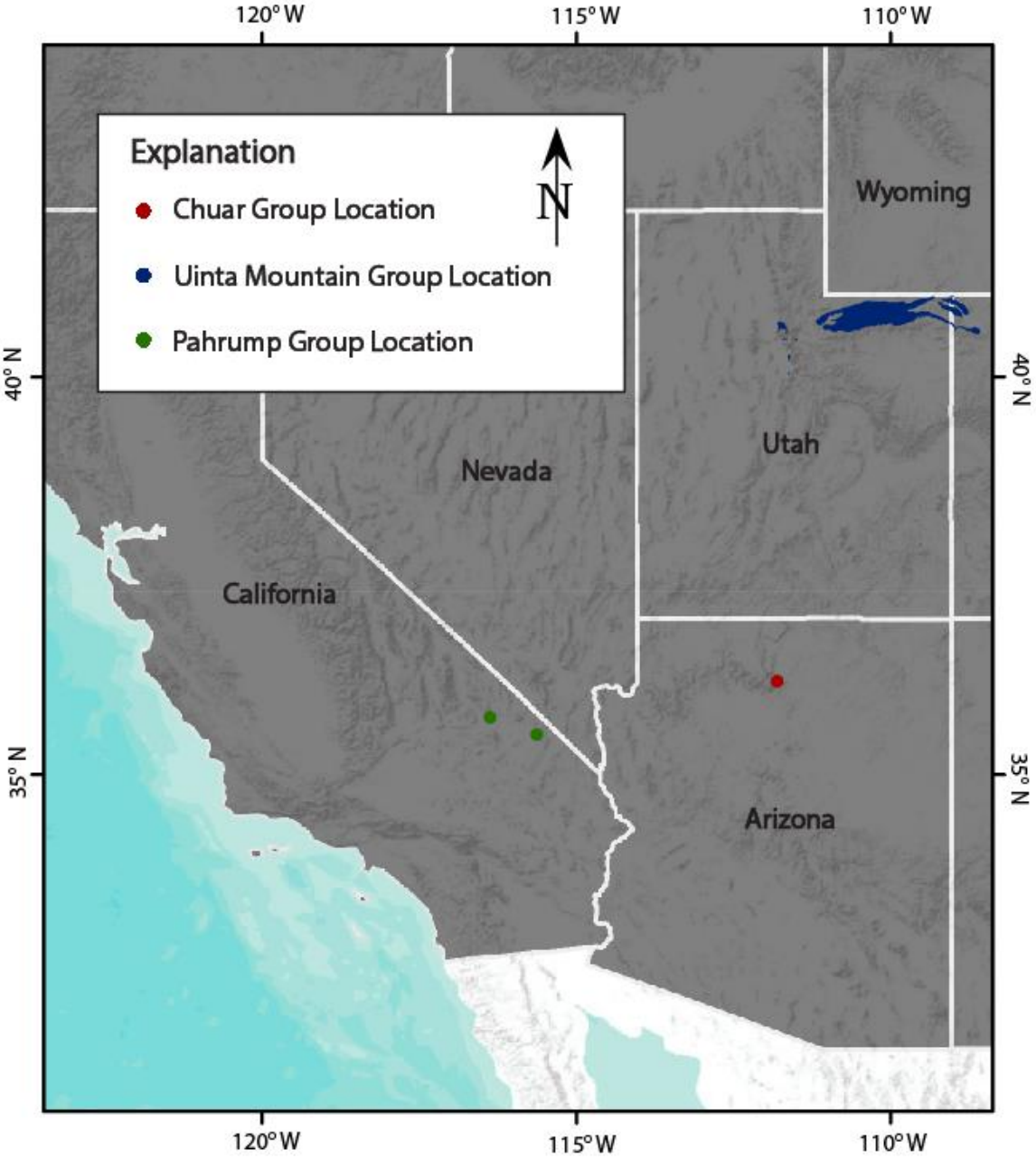

Fig. 1: *Location map of the ChUMP units. Red is the location of the Chuar Group, Grand Canyon; blue is the mapped extent of the Uinta Mountain Group, NE Utah; and green is the location of the Pahrump Group, Death Valley California.*

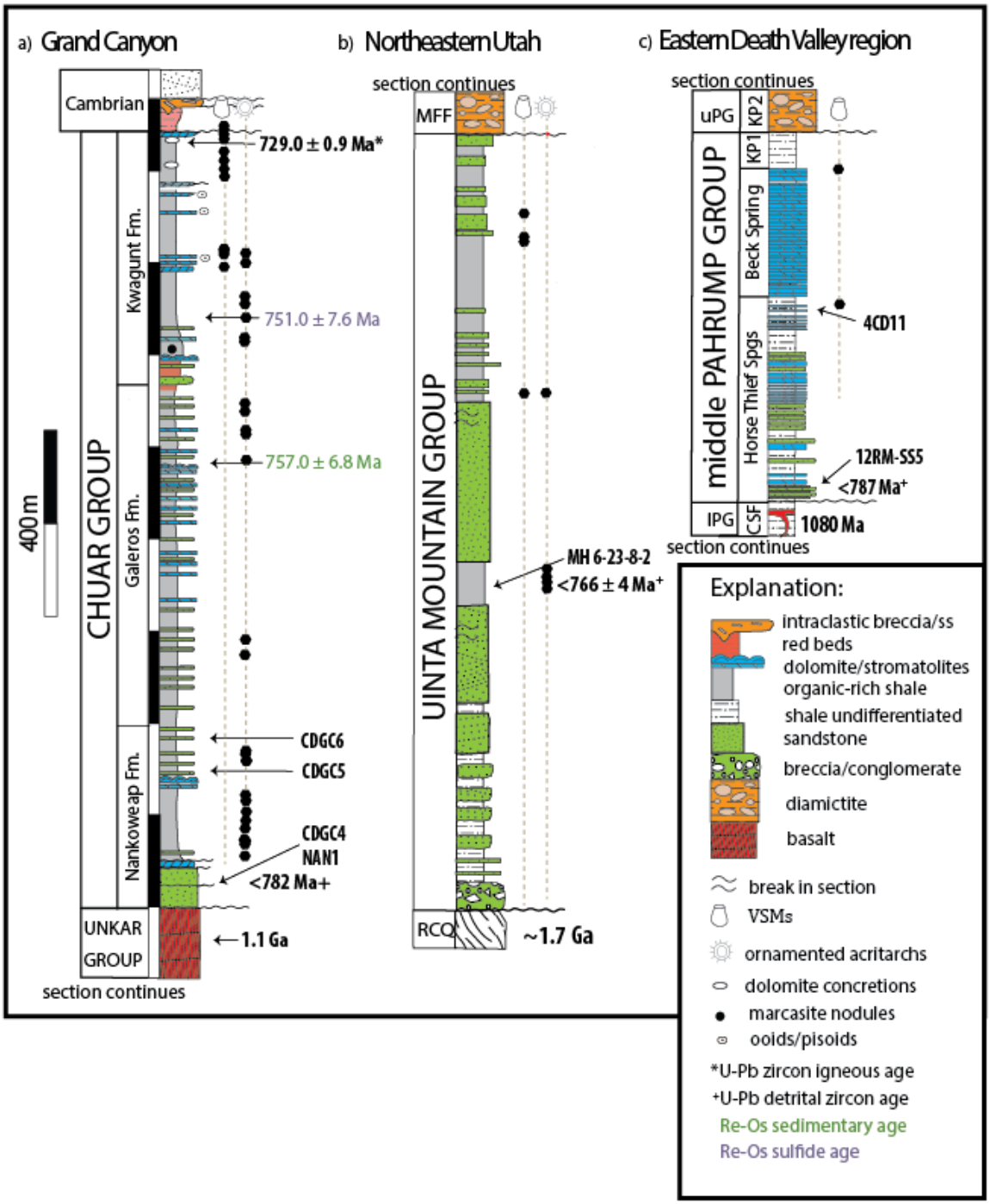

Fig. 2: *ChUMP stratigraphic column with microfossil occurrences, previous geochronology, and stratigraphic positions of samples. Modified from Dehler et al., 2017.*

The Chuar Group has a rich sedimentologic and fossil record indicating marine, restricted marine, and possible non-marine deposition. Facies are dominated by organic-rich shale, stromatolitic and laminated dolomite, and crossbedded sandstone (Dehler et al., 2001). Lesser red shale and sandstone are present in the middle Chuar Group, however, these units also contain some microfossils.

The Chuar Group contains diverse Chuar microfossils, including both ornamented and smooth-walled acritarchs, as well as vase-shaped microfossils and testate amoebae (Porter and Knoll, 2000; Riedman and Porter, 2016). Chuar Group fossils show evidence for predation at ~ 760 Ma (Porter, 2016), signifying advancement in food web complexity by this time in Earth history.

Previous work constrains the deposition of the Chuar Group to ca.782 – 729±0.9 Ma. There is a U-Pb igneous zircon age constraining deposition at the top of the Chuar Group of 729±0.9 (U-Pb TIMS), which was generated from a reworked ash bed (Karlstrom et al., 2000; Rooney 2017). Rooney et al. (2017) obtained a Model 1 Re-Os age of 757.0 ± 6.8 Ma from organic-rich carbonates of the Carbon Canyon Member, and Awatubi Member marcasite nodules yielded A Model 1 age of 751.0 ± 7.6 Ma. Dehler et al. (2017) identified 11 detrital zircon grains from the Nankoweap Fm (**Table 1**) ranging in age from 763±21 to 832±13 Ma. They interpreted the maximum depositional age to be ~ 782 Ma based on the peak in age probability (**Fig. 3**).

Table 1
Tandem LA-ICP MS of Chuar Group Zircons

Sample (a)	spot (h)	$^{206}Pb/^{238}U$ (h)	± (h)	source
CDGC4-z1	565	736	60	BSU ChUMP v2
CDGC4-z3	582	790	40	BSU ChUMP v2
CDGC4-z4	587	803	34	BSU ChUMP v2
CDGC4-z5	595	780	39	BSU ChUMP v2
CDGC4-z6	598	805	47	BSU ChUMP v2
CDGC4-z7	645	741	52	BSU ChUMP v2
CDGC4-z8	151	824	66	BSU ChUMP v3
CDGC4-z9	277	772	54	BSU ChUMP v3
CDGC4-z10	311	759	49	BSU ChUMP v3
CDGC4-z11	328	813	37	BSU ChUMP v3
CDGC4-z12	330	833	85	BSU ChUMP v3
CDGC4-z13	336	803	50	BSU ChUMP v3
CDGC5-z2	17	787	24	Arizona
CDGC5-z3	31	-	-	Arizona
CDGC5-z4	39	-	-	Arizona
CDGC5-z6	62	779	22	Arizona
CDGC5-z7	79	-	-	Arizona
CDGC5-z9	94	-	-	Arizona
CDGC6-z1	5	794	76	Arizona
CDGC6-z2	24	1966	76	Arizona
NAN1-z1	44	778	24	Arizona

(a) z1, z2 etc. are labels for single zircon grains or fragments annealed and chemically abraded after Mattinson (2005).

Uinta Mountain Group, Northern Utah

The Uinta Mountain Group (UMG) is a 4-7 km thick siliciclastic succession located in north-central Utah (**Fig. 1, Fig. 2**). The UMG and correlative Big

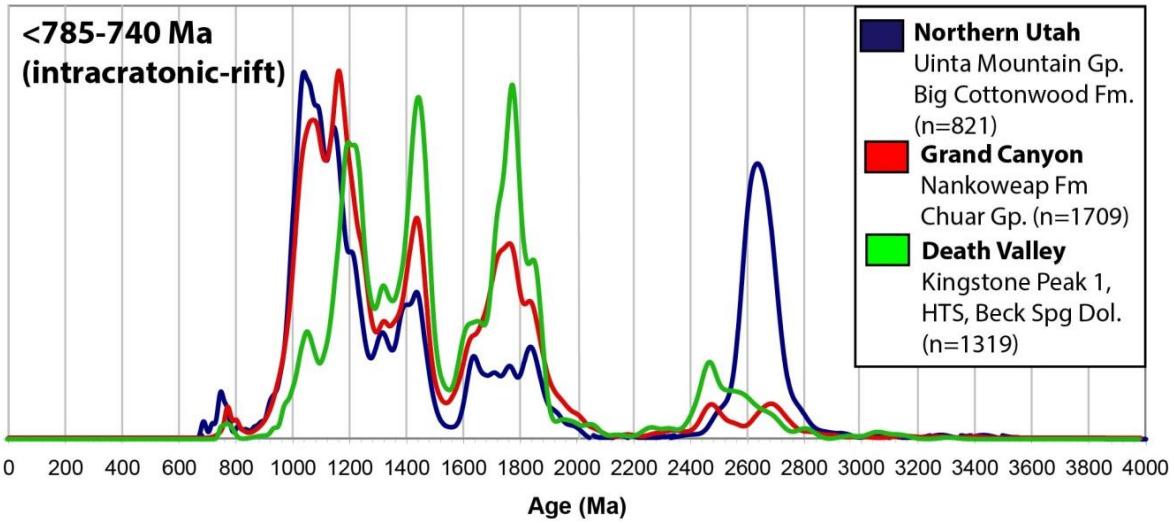

***Fig. 3**: Detrital zircon probability density plot modified from Dehler et al., 2017. The plot shows the spread of detrital zircon ages found in the Uinta Mountain Group (blue), the Chuar Group (red), and the Pahrump Group (green). The horizontal axis indicates the ages of the grains, while the vertical axis indicates the proportion of grains analyzed of a particular age in each sample. The higher the peak, the more zircons that were found to have that age. The peak at ~780 Ma that occurs in samples from all three of the ChUMP localities is the evidence that prompted this study.*

Cottonwood Formation exposures span about 65 km N-S and 300 km E-W between Salt Lake City and the Colorado-Utah border. The UMG unconformably overlies the Paleoproterozoic Red Creek Quartzite (~1650 Ma, Nelson et al. 2011) and is split informally into the eastern UMG and the western UMG, due to differences in the stratigraphy and sedimentology across the unit (Hansen, 1965; Sprinkel, 2006; Dehler et al., 2010).

The western UMG (> 4 kilometers thick) is a succession of cross-bedded orthoquartzite and sandstone, siltstone, and shale. The base is in no place exposed and it is unconformably overlain by Cambrian or Mississippian strata (Sprinkle, 2006; Dehler et al 2010). The unit of interest in this study (since it provided

zircons), the Moosehorn Lake formation (150-300 meters), is the lowermost unit in the succession. It is olive-green to yellow-green shale, with thin-medium interbeds of arkosic and quartz arenite. The unit displays ripple marks, mud cracks, bar forms, and soft-sediment deformation. It is sharply overlain by the Mount Watson Formation (< 1 km thick), which is a quartz to arkosic arenite with many types of crossbedding and bar forms (Wallace and Crittenden 1969; Wallace, 1972). The topmost unit, the Red Pine Shale (<1.8 km thick), caps 3 km of Hades Pass quartzite and is dominantly organic-rich shale containing vase-shaped microfossils and acritarchs (Dehler et al., 2007; Dehler et al., 2017). The western UMG represents fluvio-deltaic, estuarine and offshore marine environments (Wallace and Crittenden, 1969; Dehler et al., 2007; Dehler et al. 2010).

The eastern UMG (< 7 km thick) is a succession of breccia, conglomerate, lithic, quartz, and (or) feldspathic arenite, siltstone, and shale. The Outlaw Trail formation (< 300 m thick), the unit of interest in this study (as it was the lowermost unit to produce a significant number of datable zircons), is a distinctive fine-grained interval that is sandwiched between very thick arenite units of the underlying Diamond Breaks formation (<1 km thick) and overlying Crouse Canyon formation (< 3.2 kms thick) (DeGrey and Dehler, 2005; Dehler and Sprinkel, 2005; Dehler et al., 2007; Sprinkel, 2006). The Outlaw Trail formation is dominated by green shale and siltstone with interbeds of quartz arenite, sublithic arenite, and lithic arenite. The unit possesses crossbedding and bar form types. The eastern UMG represents deposition under fluvial, alluvial, deltaic, and estuarine conditions (Dehler et al.,

2010). The Outlaw Trail formation in the east is tentatively correlated with the Moosehorn Lake formation in the west based upon stratigraphic position, lithology, and preliminary detrital zircon studies (Dehler et al., 2010).

The UMG basin formed ~500 km inboard of the western Laurentian margin on entirely Laurentian crust during the breakup of Rodinia (Condie et al., 2001; Weil et al., 2006). UMG sediments were deposited in an intracratonic extensional basin that had an E-W trending northern basin margin (Mueller & Frost, 2006). The western and southern margins of the basin were open to the ocean, documented by tidal rhythmites in the Hades Pass quartzite and the correlative Big Cottonwood Fm. in the Wasatch Range to the west (Ehlers, 1999; Ehlers and Chan, 1999) and by fining and thickening of the UMG to the south (Dehler et al., 2010). Paleomagnetic data indicate a paleo-latitude near the equator (Weil et al., 2006).

Dehler et al. (2010) reported a U-Pb detrital zircon maximum depositional age of 766.4 ± 4.8 Ma from the Outlaw Trail formation (SCUMG-9) of the lower-middle UMG based on U-Pb detrital zircon SHRIMP analyses (**Table 2; Fig. 2**) Detrital zircons younger than 800 Ma were also found in the Moosehorn Lake formation (sample 73PL05) with zircons as young as 792 ±10 Ma, 761 ± 8 Ma, and 730 ± 8 Ma, and the Jesse Ewing Canyon Formation (sample 91PL05) with ages of 781 ± 10 Ma and 753 ± 12 Ma (Dehler et al. 2010).

Table 2
Tandem LA-ICP MS of Uinta Mountain Group Zircons

Sample (a)	spot (h)	$^{206}Pb/^{238}U$ (h)	± (h)	source
MH6-23-6-z4	107	705	22	Arizona
OTDZ-1-z1	24	707	27	Arizona
OTDZ-1-z2	92	783	28	Arizona
OTDZ-1-z3	27	564	26	Arizona

(a) z1, z2 etc. are labels for single zircon grains or fragments annealed and chemically abraded after Mattinson (2005).

Pahrump Group, Death Valley California

The Pahrump Group (ca. 1300-635 Ma; ~4 km thick) is exposed in the Death Valley and greater Mojave Desert area (**Fig. 1**) (Wasserburg et al., 1959; Labotka et al., 1980). It unconformably overlies the crystalline basement (1.8 – 1.2 Ga) (Roberts, 1976) and is overlain by the Marinoan Noonday Dolomite, which is the cap-carbonate unit indicating deglaciation from Snowball Earth conditions at 635 Ma (Hoffman et al., 1998; Petterson et al., 2011).

The Neoproterozoic Horse Thief Springs Formation (< 650 meters), the unit of interest in this paper, rests in disconformity and angular unconformity with the underlying Mesoproterozoic Crystal Spring Fm. (Maud, 1979), with a duration of lost time that spans at least 300 m.y. (Mahon et al., 2014). The Horse Thief Springs Formation is a mixed siliciclastic-carbonate unit that is cyclic and grades upwards into the Beck Spring Dolomite (Error! Reference source not found.). Vase-shaped

microfossils are found near the base and at the top of the HTS (unit B and unit F of Maud (1979) (Horodyski, 1993; Dehler, 2014; Mahon et al., 2014).

Mahon et al. (2014) presented a maximum depositional age of 787 ± 11 Ma for the basal Horse Thief Springs Formation based on LA-ICP-MS U-Pb detrital zircon analyses (**Table *3***) of Neoproterozoic grains (n = 6) across 4 samples (Error! Reference source not found.). Two "young" (Neoproterozoic) grains each were recovered from samples K03DV10 (786 ± 19 Ma and 760 ± 6) and K03DV11 (802 ± 11 Ma and 785 ± 11), which were taken < 12 m above the unconformity. Samples 12RMSS5 (same locality as K03DV10 and K03DV11) and 4CD11 (unit F of the formation in the Kingston Range) each contained a single "young" grain, ages 780 ± 17 and 774 ± 10

Table 3:
Tandem LA-ICP MS of Pahrump Group Zircons

Sample (a)	spot (h)	$^{206}Pb/^{238}U$ (h)	± (h)	source
12RM-SS5-z1	232	801	27	BSU ChUMP v2
12RM-SS5-z2	18	823	34	BSU ChUMP v3
12RM-SS5-z3	37	917	45	BSU ChUMP v3
12RM-SS5-z4	94	787	52	BSU ChUMP v3
12RM-SS5-z5	58	786.2	33.8	Mahon et al., 2014
12RM-SS5-z6	174	998	82	BSU ChUMP v2
12RM-SS5-z7	212	1001	107	BSU ChUMP v3
12RM-SS5-z8	203	1068	289	BSU ChUMP v3
4CD-11-z1	27	873		Arizona
4CD-11-z2	30	772	94	Mahon et al., 2014
4CD-11-z3	66	889		Arizona
4CD-11-z4	98	612		Arizona

(a) z1, z2 etc. are labels for single zircon grains or fragments annealed and chemically abraded after Mattinson (2005).

Ma, respectively. Mahon et al. (2014) found the weighted mean of ages for these grains to be 775 ± 18 Ma. With an outlier excluded, they acquired a mean age of 787 ± 11Ma, which is a more conservative estimate for the maximum age of deposition (Mahon et al., 2014).

ChUMP Correlation and Significance

The **Ch**uar, the **U**inta **M**ountain, and the middle **P**ahrump (starting at the base of the Horse Thief Springs formation) groups have several similarities. These units indicate coeval intracratonic basin formation and a flooded craton at ca. 780 Ma. They show evidence of tectonic activity in an extensional setting, and are likely related to an early phase of the rifting of Rodinia. The units provide a record of the ~50 Mys leading to the onset of global glaciation, are bounded by unconformities, and have age constraints between ca. 780 and ca. 730 Ma. Evidence is mounting that strata of the Chuar, Uinta Mountain, and Pahrump Groups are not just similar to one another: they are essentially the same rocks (Maud, 1979; Timmons et al., 2001; Dehler et al., 2010; MacDonald et al., 2010; Li et al., 2013; Kingsbury-Stewart et al., 2013; Mahon et al. 2014; Dehler et al., 2017).

Further evidence linking the ChUMP units and indicating their significance is found in their fossil records and carbon-isotope values. Vase-shaped microfossils appear in all three units (Horodyski, 1993; Porter and Knoll, 2000; Dehler et al., 2007; Dehler, 2014). Both the lower Chuar and Uinta Mountain groups possess similar diverse ornamented acritarch assemblages indicating a notable rise in

eukaryotic diversity by the time the basal formations were deposited (Porter and Riedman, 2016). Chuar Group microfossils show evidence for predation at 760-730 Ma, signifying the advancement in food web complexity by this time in Earth history (Porter and Knoll, 2000; Porter, 2016). Along with these important biological innovations, carbon-isotope values in the ChUMP groups show large-scale variability, indicating long-term changes in the global burial rates of carbon (Dehler et al., 2001; Dehler et al., 2010; Smith et al., 2015; Dehler et al., 2017).

U-Pb Geochronology

Three stable Pb isotopes are the ultimate products of three complex decay chains stemming from U and Th. The intermediate members of these series are short-lived, so much so that they are of negligible importance on a timescale of millions of years. The half-life from parent to final daughter varies drastically between the three systems. ^{235}U has the shortest, with a duration of about 0.704 billion years passing before half of the parent decays into ^{207}Pb. The half-life for ^{238}U to ^{206}Pb is 4.47 billion years, and for ^{232}Th to ^{208}Pb it is 14.01 billion years (Dicken, 2005).

Pb and U are highly mobile when subject to low-grade metamorphism. This leads to most U-Pb systems opening at some point during a rock's existence, allowing for Pb to escape the system. The U-Pb system is nevertheless useful due to the existence of two separate decay schemes, $^{206}Pb/^{238}U$ and $^{207}Pb/^{235}U$. When the ratios of parent and daughter isotopes from both decay schemes are plotted against

one another, the robustness of an age can be extrapolated using a concordia plot. If the system has not experienced Pb loss, the isotopic ratios from the two systems will fall along a predictable curve, known as the concordia curve, which is the point where the $^{206}Pb/^{238}U$ age equals the $^{207}Pb/^{235}U$ age. The curve is generated so that the ratios are proportional to time. If the ratios plot below the concordia line, lead loss has occurred. Since Pb is lost at a predictable rate, if ages are obtained for multiple zircons, they will plot in a curve below the concordia line. That curve, if extrapolated upward to where it intersects with the concordia line, provides an upper-intercept age approximating the true age of the zircon (Dicken, 2005). If a ratio plots above the Concordia line it suggests that lead has found its way into the system. This does not naturally occur, and is far more likely to indicate an error in the methodology than it is to indicate lead gain.

While many of the zircons in this study had never been analyzed previously, 37 of the zircons are from 'legacy mounts', which were already subject to LA-ICP-MS at University of Arizona's Laserchron Lab. LA-ICP-MS utilizes laser ablation to excavate a pit in the zircon. A stream of helium gas carries the material from the pit to the ICP-MS where it undergoes ionization by the plasma. The electromagnetic field separates the isotopes of U and Pb so that their amounts are measured independently of one another. During the transition to the ICP-MS many ions are lost, introducing error to the process. LA-ICP-MS also does not discriminate between what it ionizes. As a result, the measurement may not represent the chemistry of the zircon itself, but rather that of an inclusion within the grain, an overgrowth that is

the product of zoning, or a portion of the grain that has experienced Pb loss (Feng et al., 1993). This method provided data suitable for the purposes of Mahon et al. (2014), and Dehler et al. (2017), but these ages lack the precision that can be achieved with CA-ID-TIMS.

Another precursor to this study, Dehler et al. (2010), utilized Sensitive High-Resolution Ion MicroProbe (SHRIMP). SHRIMP utilizes a Secondary Ion Mass Spectrometer (SIMS) to generate a beam of ions that are focused on the surface of the zircon to produce ions. These ions are transferred to a mass spectrometer, where they are analyzed. It is extremely time intensive and expensive (Hinton, 1995). The zircons from Dehler et al. (2010) were unavailable for reevaluation in the timeframe necessary for them to be included in the project.

METHODS

Sample Acquisition

Mid-Neoproterozoic grains were plucked from mounts previously analyzed via LA-ICP-MS at University of Arizona's Laserchron Facility (Mahon et al. 2014; Dehler et al. 2017; unpublished data). To supplement the small sample pool of Neoproterozoic zircons within the ChUMP legacy mounts, additional archived rock samples were mechanically and chemically separated and analyzed for additional mid-Neoproterozoic zircons using the LA-ICPMS at Boise State University. Both random and non-random samplings of zircons were taken for each sample being re-analyzed. For the non-random sampling, we searched for grains that were euhedral crystals, which indicate that they have been eroded less during their transport history and are therefore more likely to be young.

Three legacy mounts from the Nankoweap Formation (Dehler et al., 2017) were used (CDGC5, CDGC6, NAN-1; quartz arenite) and one new mount (CDGC4; quartz arenite) was made. All samples are from within a measured section in Nankoweap Canyon (Dehler et al., 2017; Appendix A; **Table 4**).

Two legacy mounts from the Uinta Mountain Group (unpublished data) were used: one from the Moosehorn Formation (MH6-23-08; quartz arenite) of the basal UMG in the western Uinta Mountains, and one from the Outlaw Trail formation of the lower-middle UMG in the eastern Uintas (OTDZ-1; subfeldspathic arenite) (Appendix A).

Table 4

Detrital zircon sample localities and sources

ChUMP Succession	Sample Name	Formation	Locality	UTM Coordinates	Source Study
Chuar	CDGC4	Nankoweap Fm.	Nankoweap Canyon, Grand Canyon, AZ.	12S 0419918 4015852	Dehler et al. 2017
Chuar	CDGC5	Nankoweap Fm.	Nankoweap Canyon, Grand Canyon, AZ.	12S 0419918 4015852	Dehler et al. 2017
Chuar	CDGC6	Nankoweap Fm.	Nankoweap Canyon, Grand Canyon, AZ.	12S 0419918 4015852	Dehler et al. 2017
Chuar	NAN1	Nankoweap Fm.	Nankoweap Canyon, Grand Canyon, AZ.	12S 0419918 4015852	Dehler et al. 2017
Uinta Mountain	Moosehorn 6-23-8-2	Moosehorn Lake Fm.	Slate Gorge, Mirror Lake Highway, Uintas, UT.	12S 0504138 4498612	Dehler unpublished
Uinta Mountain	OTDZ-1	Outlaw Trail Fm.	Browns Park, UT.	--	--
Pahrump	12RMSS5	Horse Thief Springs Fm. A unit	Saratoga Spring, Death Valley Nat'l Park, CA.	11S 0552634 3949335	Mahon 2014
Pahrump	4CD11	Horse Thief Springs Fm. F unit	Crystal Spring, Kingston Range, CA.	11S 06030506 3957264	Mahon 2014

Two legacy mounts from the Horse Thief Springs Formation (Mahon et al., 2014) were used along with three new mounts. Sample 12RMSS-5 (white quartzite) is from the basal Horse Thief Springs Formation, Saratoga Springs, Death Valley and is known to contain mid-Neoproterozoic grains (Mahon et al., 2014). A legacy mount was used and three new mounts were made of this sample. The other HTS legacy mount, 4CD11, is from a silty arenite (F-unit) taken at the HTS-Beck Spring contact (Maud, 1979) (**Fig.2**, Appendix A).

Data Acquisition

The finished mounts were carbon coated, which allows the grains to be imaged within the scanning electron microscope (SEM), and imaged at either 200x or 350x magnification. The grains were loaded into the LA-ICP-MS. One analysis was taken on each grain in order to obtain an age for each grain in the study. The spot size was 25 microns, with the laser repetition at 10 Hertz.

Zircons that provided ages close to the mid-Neoproterozoic target age and were concordant were plucked from their mounts and prepped for TIMS.

Abrasion, dissolution, and CA-ID TIMS

The remaining zircon grains were annealed and chemically abraded according to the methods of Mattinson (2005) and Davydov (2010). Briefly, zircons were annealed via heating, stabilizing lattice radiation damage. The zircons were chemically dissolved over multiple steps using HF, and spiked with EARTHTIME mixed ^{205}Pb-^{233}U-^{235}U tracer solution. U and Pb were separated from the zircon

matrix and dried with H_3PO_4 before being loaded onto a single outgassed Re filament. These steps removed zircon zones with high U+Th concentrations, leaving only the portion of the grain that had experienced little-to-no Pb loss.

U and Pb isotopic measurements were made on an IsotopX GV Isoprobe-T multicollector TIMS, which is equipped with an ion-counting Daly detector. Calculations on U-Pb data were undertaken using Isoplot 3.0 (Craddock et al., 2016).

RESULTS

Of the detrital zircons taken from the mounts of previous studies and generated from new processing of rock from previous field samples, only 21 Chuar grains, 4 Uinta Mountain grains, and 12 Pahrump grains were chosen for ID-TIMS testing and subsequently produced measurable results after the dissolution process.

Of the twenty-one grains from the Nankoweap Formation, four yielded $^{206}Pb/^{238}U$ isotopic ages in excess of 1000 Ma, making them much older than the known maximum depositional age of the Nankoweap Fm. One grain yielded an isotopic age of 800.66 ± 0.54 (**Table 5, Fig. 4**). This is within the margin of error of the previous analysis (794 ± 76 Ma). The remaining 16 grains yielded concordant isotopic ages between 780 and 770 Ma, with 11 yielding ages between 776.04 ± 0.98 Ma and 774.99 ± 1.54 Ma. These strongly concordant ages are 6-7 My younger than Dehler et al. (2017) reported. These zircons came from samples ~34 meters (CDGC4) and 70 meters (CDGC5) above the base of the Nankoweap. Most of them are rounded to sub-rounded. Further descriptions and images of these grains are located in Appendix B. The single zircon yielding a concordant age of 770.10 ± 0.48 is considered unreproducible.

Of the four grains from the Uinta Mountain Group that were analyzed via CA-ID TIMS, three of them came from the eastern UMG Outlaw Trail sample (OTDZ-1). These grains yielded concordant $^{206}Pb/^{238}U$ isotopic ages of 892.84 ± 0.58 Ma, 765.82 ± 0.56 Ma, and 592 ± 0.59 Ma (**Table 6, Fig. 5**). The oldest of these

Table 5

CA-ID TIMS Isotopic Ages of Chuar Group Zircons

Sample (a)	$^{207}Pb/^{206}Pb$ (g)	± (f)	$^{207}Pb/^{235}U$ (g)	± (f)	$^{206}Pb/^{238}U$ (g)	± (f)
CDGC4-z1	765.71	14.61	773.01	4.19	775.53	1.44
CDGC4-z3	776.95	9.31	776.28	2.73	776.04	0.98
CDGC4-z4	770.57	6.04	774.17	1.91	775.42	1.03
CDGC4-z5	770.97	9.52	774.51	2.83	775.74	1.22
CDGC4-z6	777.79	14.37	776.84	4.14	776.51	1.34
CDGC4-z7	770.75	15.25	773.90	4.38	774.99	1.54
CDGC4-z8	763.97	9.22	772.32	2.86	775.21	1.64
CDGC4-z9	776.37	5.87	775.92	1.79	775.76	0.76
CDGC4-z10	782.74	7.85	779.50	2.39	778.36	1.06
CDGC4-z11	779.25	8.35	776.34	2.48	775.33	0.89
CDGC4-z12	769.17	13.39	773.77	4.04	775.36	2.13
CDGC4-z13	774.15	6.04	775.37	1.86	775.79	0.81
CDGC5-z2	773.17	2.96	770.89	1.07	770.10	0.48
CDGC5-z3	1863.2	1.5	1861.9	1.7	1860.7	2.3
CDGC5-z4	1056.7	19.6	1062.2	7.6	1064.9	4.9
CDGC5-z6	773.31	5.16	775.20	1.65	775.86	0.83
CDGC5-z7	1086.0	2.7	1079.8	1.3	1076.8	0.9
CDGC5-z9	767.87	8.06	773.52	2.41	775.48	0.96
CDGC6-z1	801.53	2.67	800.89	0.99	800.66	0.54
CDGC6-z2	1104.2	2.7	1087.7	1.3	1079.4	0.7
NAN1-z1	772.37	8.49	774.51	2.52	775.26	0.82

(a) z1, z2 etc. are labels for single zircon grains or fragments annealed and chemically abraded after Mattinson (2005).
(f) Errors are 2-sigma, propagated using the algorithms of Schmitz and Schoene (2007).
(g) Calculations are based on the decay constants of Jaffey et al. (1971). 206Pb/238U and 207Pb/206Pb ages corrected for initial disequilibrium in 230Th/238U using Th/U [magma] = 3.

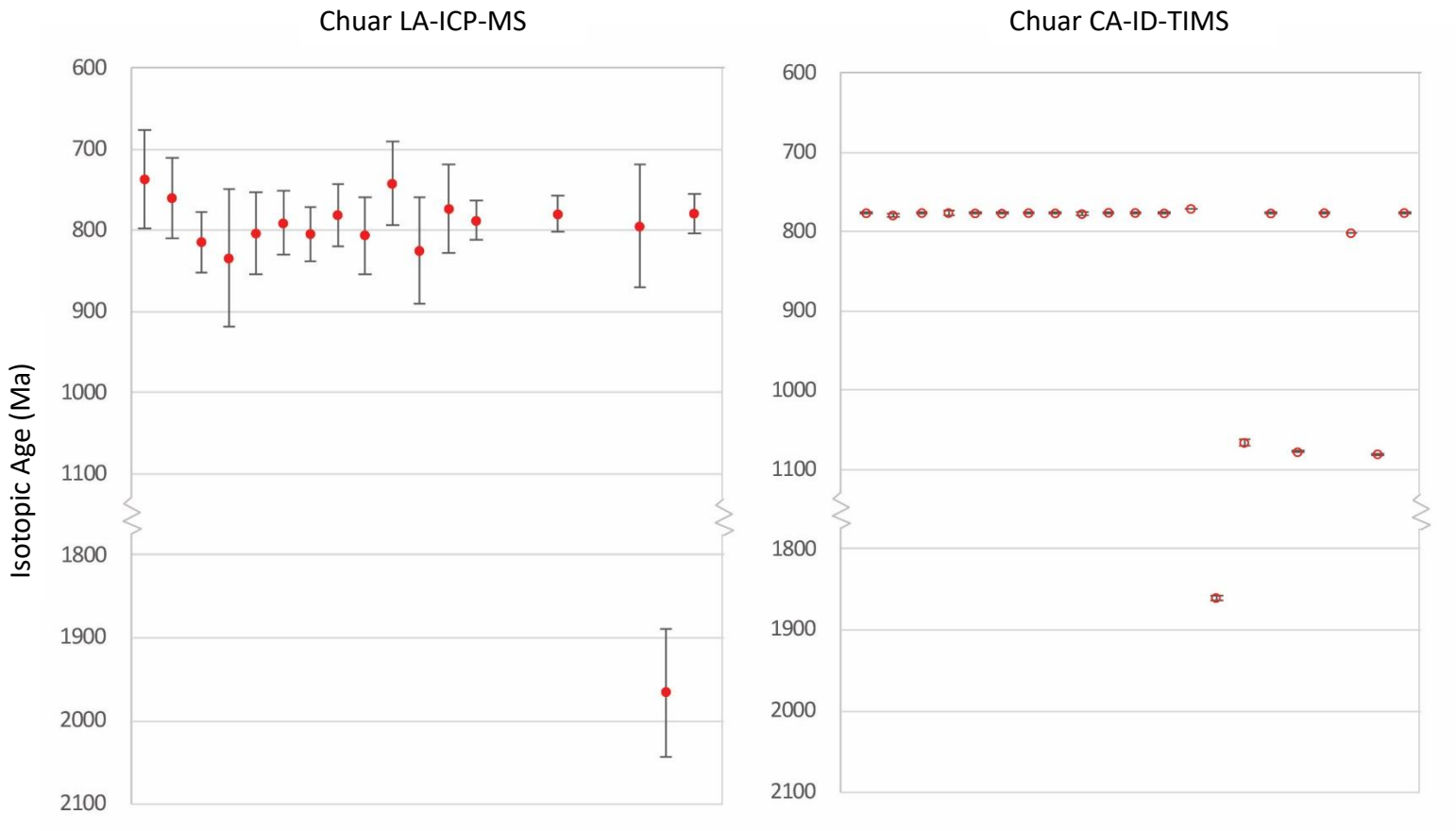

Fig. 4: *Isotopic LA-ICP-MS (left) and CA-ID TIMS (right) ages of Nankoweap Fm. zircons.*

Table 6

CA-ID TIMS Isotopic Ages of Uinta Mountain Group Zircons

Sample (a)	$^{207}Pb/^{206}Pb$ (g)	± (f)	$^{207}Pb/^{235}U$ (g)	± (f)	$^{206}Pb/^{238}U$ (g)	± (f)
MH6-23-6-z4	770.23	22.22	767.73	6.29	766.88	2.31
OTDZ-1-z1	769.78	2.38	766.83	0.90	765.82	0.56
OTDZ-1-z2	913.49	1.64	898.80	0.83	892.84	0.58
OTDZ-1-z3	594.02	4.32	592.60	1.14	592.23	0.59

(a) z1, z2 etc. are labels for single zircon grains or fragments annealed and chemically abraded after Mattinson (2005).
(f) Errors are 2-sigma, propagated using the algorithms of Schmitz and Schoene (2007).
(g) Calculations are based on the decay constants of Jaffey et al. (1971). 206Pb/238U and 207Pb/206Pb ages corrected for initial disequilibrium in 230Th/238U using Th/U [magma] = 3.

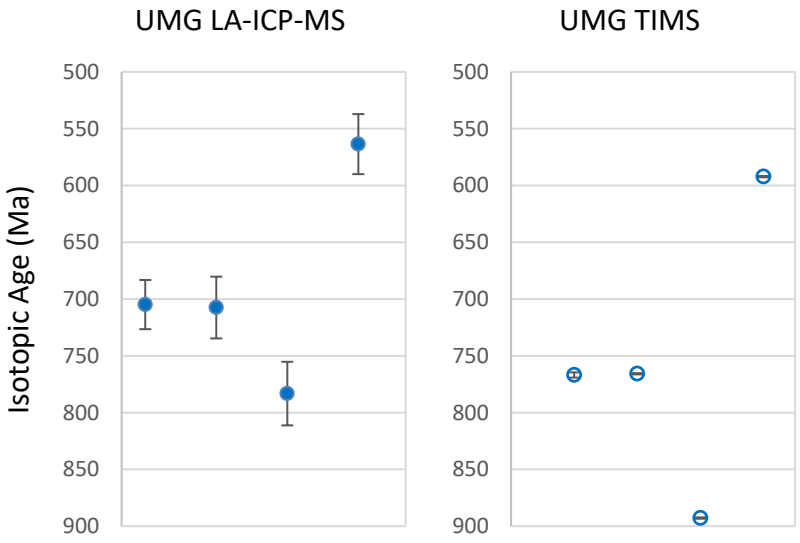

Fig. 5: *Isotopic LA-ICP-MS (left) and CA-ID TIMS (right) ages of Uinta Mountain zircons.*

exceeds the previously known maximum depositional age of the unit, while the youngest zircon provides an age within the Ediacaran, which we reject. The median age of 765.82 ± 0.56 Ma, however, mimics the Dehler et al., (2010) age of 766 ± 4.8

Ma. This sample was collected from ~2,500 meters above the base of the UMG. The fourth UMG grain is from the western UMG Moosehorn Lake formation (MH-6-23-8-2). It yields an age of 766.88 ± 2.31 Ma, which is also consistent with Dehler et al. (2010). This sample was collected from near the base of the exposed western UMG.

Four of the 12 analyzed Horse Thief Springs grains are from the Kingston Range (4CD11), and were collected ~300 meters above the base of the HTS. Three of them yielded old $^{206}Pb/^{238}U$ ages from 1427 - 1301 Ma, and the fourth grain yielded a slightly discordant age of 808.09 ± 3.61 Ma (**Table 7, Fig. 6**). The eight remaining HTS grains came from the basal HTS at Saratoga Spring (12RMSS5), from a sample

Table 7
CA-ID TIMS Isotopic Ages of Pahrump Group Zircons

Sample (a)	$^{207}Pb/^{206}Pb$ (g)	± (f)	$^{207}Pb/^{235}U$ (g)	± (f)	$^{206}Pb/^{238}U$ (g)	± (f)
12RM-SS5-z1	773.04	9.45	774.86	2.84	775.49	1.25
12RM-SS5-z2	808.10	1.50	801.99	0.73	799.79	0.49
12RM-SS5-z3	918.27	5.29	916.65	2.13	915.98	1.64
12RM-SS5-z4	777.40	8.79	775.87	2.59	775.34	0.91
12RM-SS5-z5	744.08	52.08	768.41	14.19	776.81	3.87
12RM-SS5-z6	1025.92	2.23	1021.01	1.09	1018.72	0.72
12RM-SS5-z7	990.38	2.26	931.16	1.35	906.34	1.34
12RM-SS5-z8	1065.54	3.69	1065.98	1.95	1066.19	1.77
4CD-11-z1	1301.88	13.14	1301.71	5.95	1301.61	3.99
4CD-11-z2	1427.00	11.10	1427.47	5.81	1427.78	5.17
4CD-11-z3	1306.54	13.34	1306.88	5.97	1307.08	3.90
4CD-11-z4	872.77	9.51	825.52	3.91	808.09	3.61

(a) z1, z2 etc. are labels for single zircon grains or fragments annealed and chemically abraded after Mattinson (2005).
(f) Errors are 2-sigma, propagated using the algorithms of Schmitz and Schoene (2007).
(g) Calculations are based on the decay constants of Jaffey et al. (1971). 206Pb/238U and 207Pb/206Pb ages corrected for initial disequilibrium in 230Th/238U using Th/U [magma] = 3.

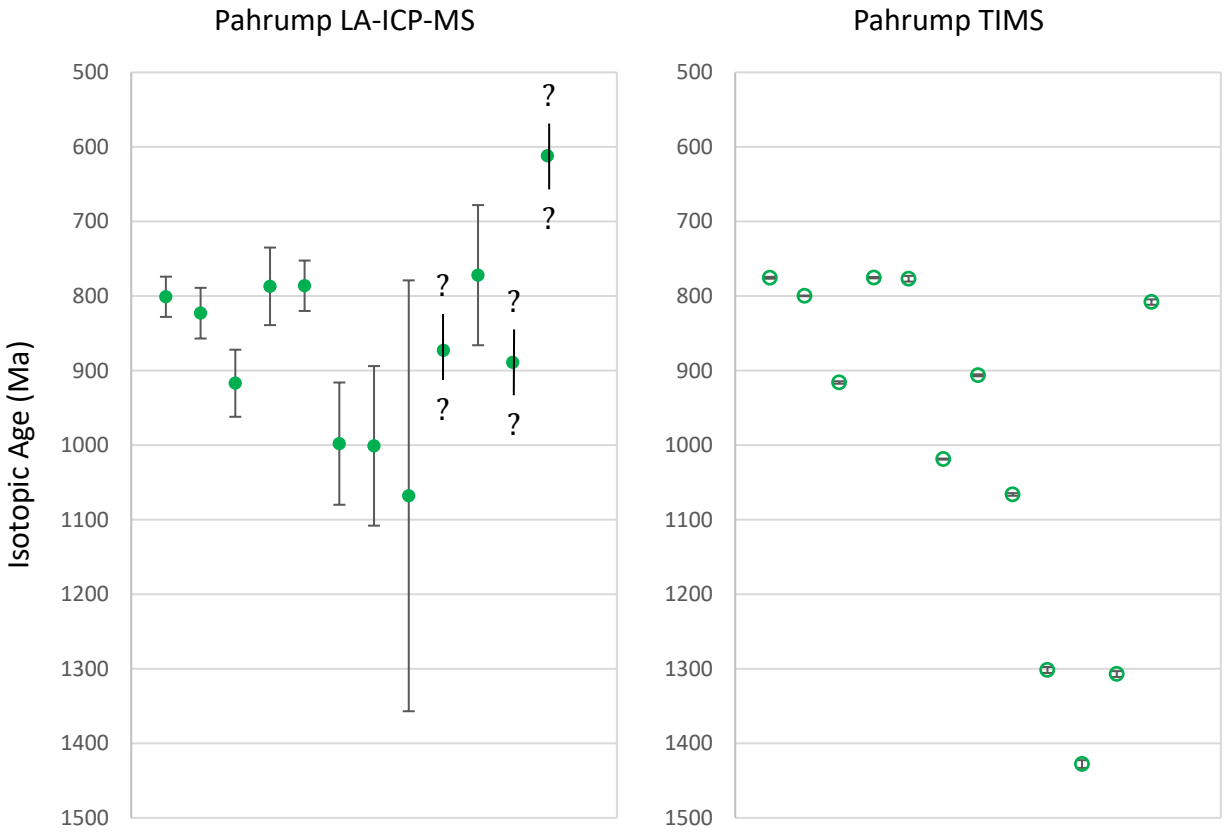

Fig. 6: *Isotopic LA-ICP-MS (left) and CA-ID TIMS (right) ages of Pahrump zircons.*

12.5 meters above the basal unconformity. Four of these yielded older $^{206}Pb/^{238}U$ ages of 1066 Ma - 906 Ma. The remaining four grains yielded concordant $^{206}Pb/^{238}U$ ages of 799.79 ± 0.49 Ma, 776.81 ± 3.87 Ma, 775.49 ± 1.25 Ma, and 775.34 ± 0.91 Ma. The new ages overlap with the previous 787 ± 11 Ma age by between 1.57 and 0.25 My. Descriptions and images of two of these zircons can be found in Appendix B. These grains are rounded to sub-rounded.

Compositional parameters for all analyzed grains are located in Appendix C, and radiogenic isotopes of the grains are located in Appendix D.

DISCUSSION

Refined Detrital Zircon Geochronology of basal ChUMP Units

Both the Horse Thief Springs Formation of the Pahrump Group and the Nankoweap Formation of the Chuar Group produce grains with concordant $^{206}Pb/^{238}U$ ages of ~775 Ma that are within analytical uncertainty of one another (**Fig. 7**). The ~775 Ma Chuar grains provided a mean age of 775.63 ± 0.27 Ma, while the ~775 Ma Pahrump grains provided a mean age of 775.44 ± 0.73 Ma.

We consider the 775.63 ± 0.27 Ma age to reduce the approximate maximum depositional age of the Nankoweap Formation as described in Dehler et al. (2017) by 7 My, as the 782 Ma age was reported without associated errors. **Fig. 8**

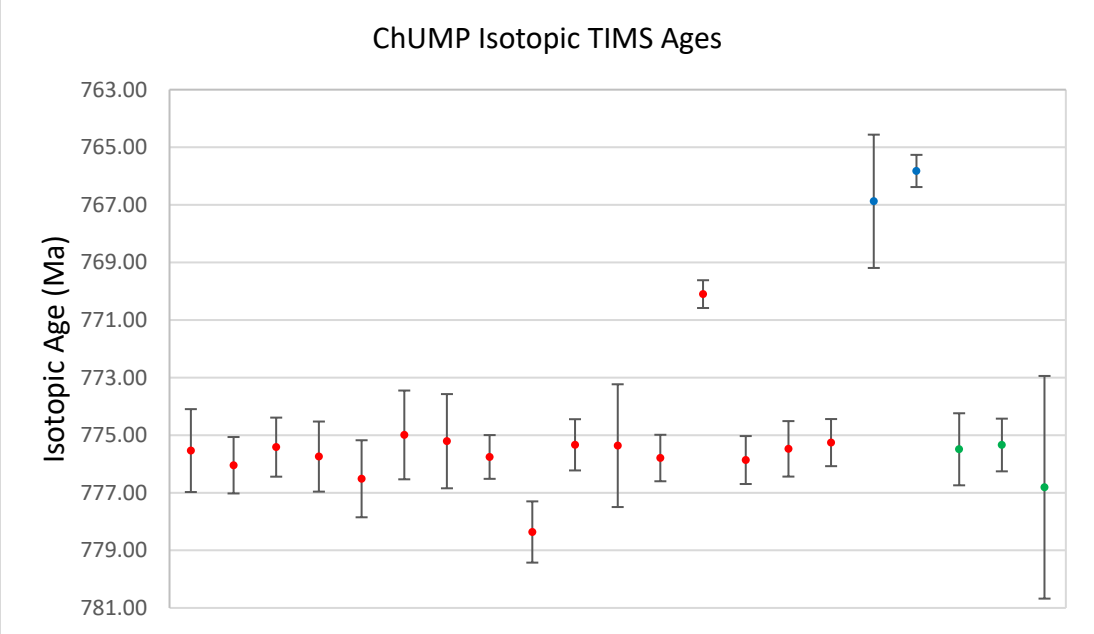

Fig. 7: *CA-ID TIMS ages and errors of ~775 Ma or younger ChUMP zircons. Chuar grains are red; Uinta Mountain grains are blue; and Pahrump grains are green*

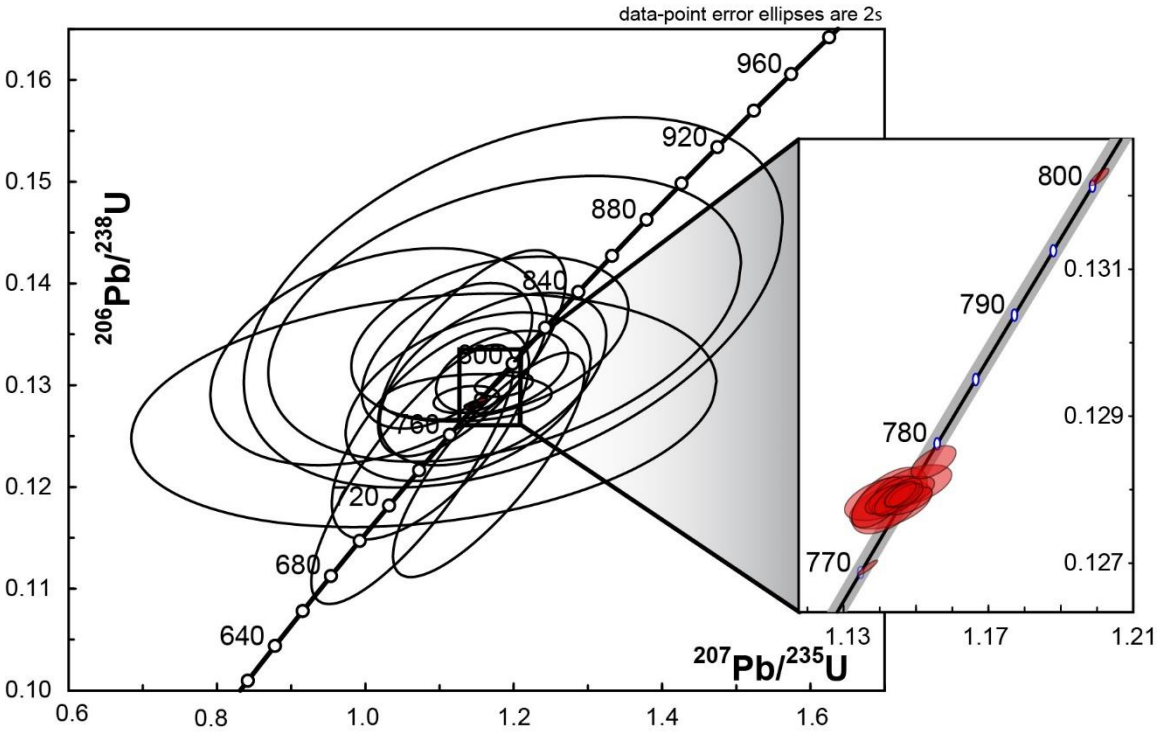

Fig. 8: *Chuar Concordia plot. White ellipses indicate LA-ICP MS ages. Red ellipses indicate the twelve refined CA-ID TIMS ages.*

demonstrates the increase in precision obtained by analyzing zircons formerly analyzed by LA-ICP-MS with ID-TIMS. Several of our CA-ID TIMS ages were obtained from grains originally analyzed in this previous study. The ages and errors associated with each grain previously left tens of millions of years in which these zircons could have formed. The ID-TIMS ages are precise and concordant.

The 775.44 ± 0.73 Ma mean age is mostly younger than the 787 ± 11 Ma LA-ICP MS maximum age reported by Mahon et al. (2014) for the Horse Thief Springs Formation (**Fig. 9**), though there is an overlap of 0.15 My. The 775.44 ± 0.73 Ma ages are concordant, especially the two for which a higher degree of precision was

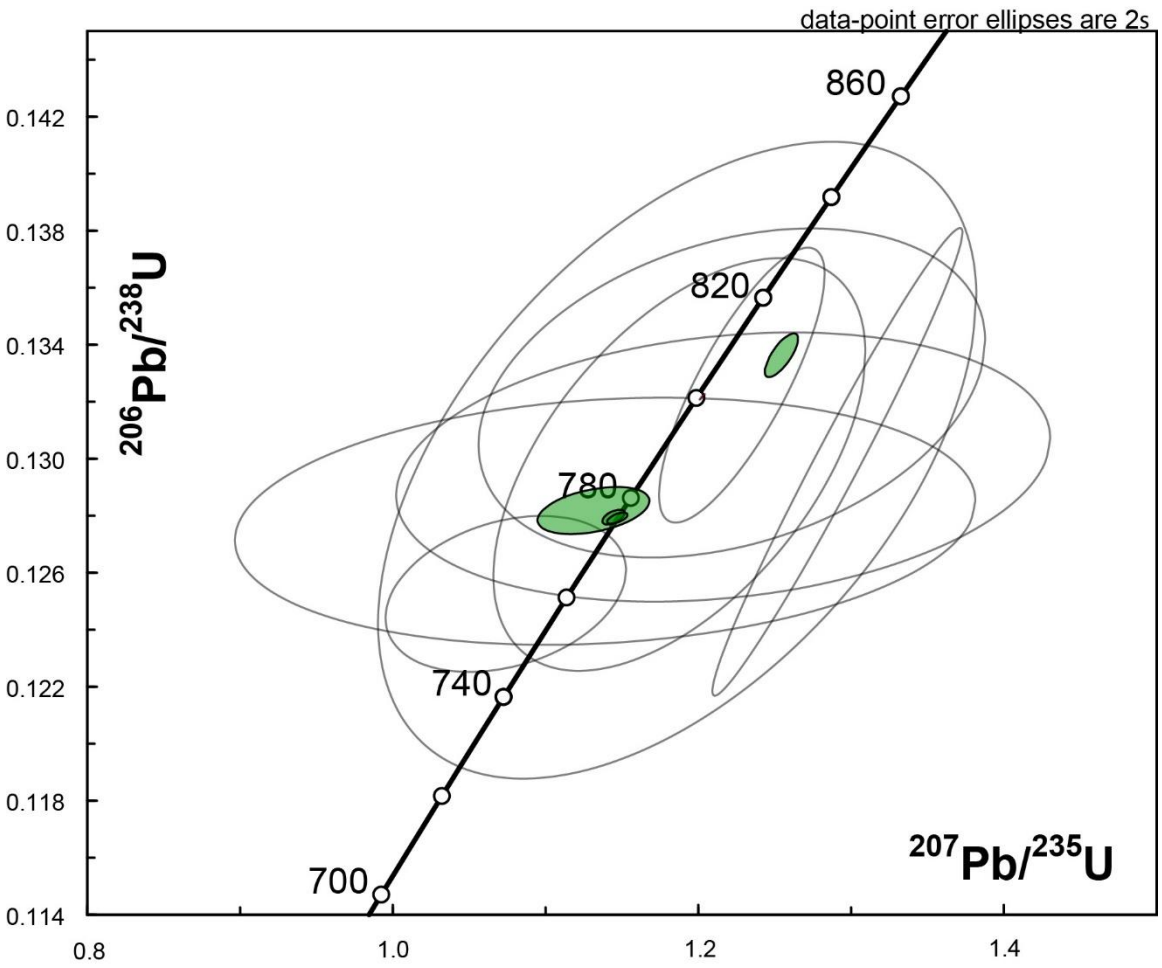

Fig. 9: *Pahrump Concordia plot. White ellipses indicate LA-ICP-MS ages. Green ellipses indicate the four refined CA-ID TIMS ages.*

obtained. **Fig. 9** further demonstrates the ability of ID-TIMS to dramatically increase the precision of a dataset originally obtained via LA-ICP-MS.

The Moosehorn Lake and Outlaw Trail formations of the Uinta Mtn. Group provided one accepted grain each. Their ages are consistent with a U-Pb SHRIMP maximum depositional SHRIMP age of 766.4 ± 4.8 Ma obtained from Outlaw Trail detrital zircons (Dehler et al., 2010), and with grains from the basal Jesse Ewing Canyon Formation that provided ages of 753 ±12 Ma and 781 ±10 Ma. It is also

consistent with geologic mapping that strongly support correlation between the two units (Sprinkel et al., 2006; Rybcyznski 2008; Dehler et al., 2010).

This study demonstrates how analyzing a non-random sampling of grains that have already been analyzed via LA-ICP MS can vastly improve the precision of age data for a population. ~4,500 zircons were analyzed during the course of the precursor studies to this project (Dehler et al., 2010; Mahon et al., 2014; Dehler et al., 2017). Using TIMS to reanalyze a specific population of zircons, in this case the few dozen that had already provided the "young" ages in their respective studies, enabled us to refine the maximum depositional age for the ChUMP strata with a precision the previous studies lacked.

Proximity of acquired ages to the age of deposition

Although the detrital age on the Nankoweap Formation obtained for this publication suggests a maximum depositional age of 775 Ma, other research can effectively provide a minimum depositional age as well. The Nankoweap Formation can be no younger than a newly reported Re-Os depositional age on an organic-rich dolostone of 757 ± 6.8 Ma obtained from the Carbon Canyon Member (Rooney et al. 2017), which is stratigraphically positioned ~700 m above the Nankoweap Formation samples (**Fig. 10**). This age allows for between 11 and 24 million years to be represented in the intervening 700 meters of strata between the sampling locations. Considering a sediment accumulation rate of 20-30 m/My for the Chuar Group (based on carbonate platform sedimentation of Sadler, 1981), it is

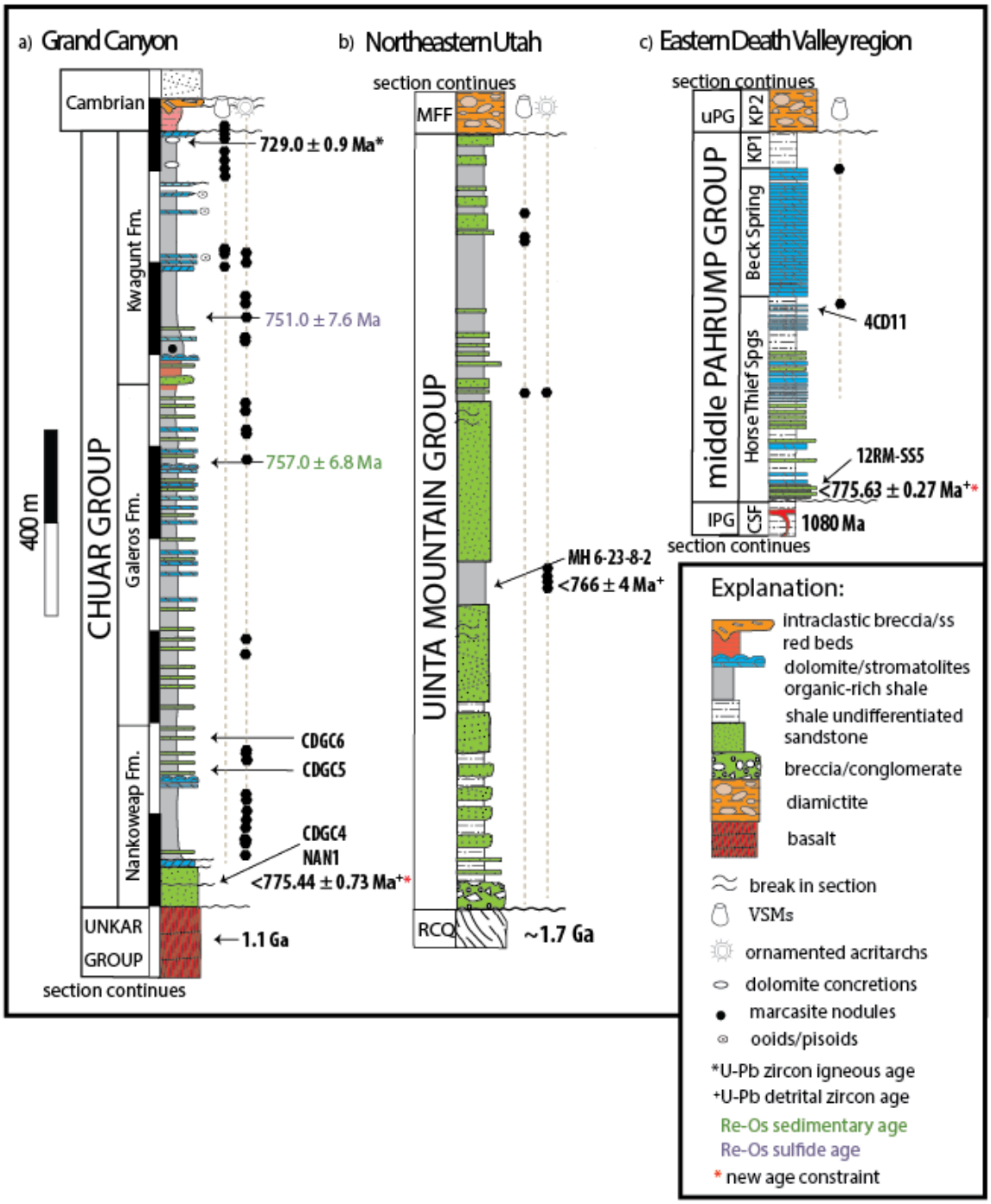

Fig. 10: *ChUMP stratigraphic column updated with new detrital zircon ages. Modified from Dehler et al., 2017.*

likely that the actual depositional age for the Nankoweap Fm. is within a few million years of the 775.63 ± 0.27 Ma maximum depositional age and reflects rift basin development and regional volcanism at this time. It also seems more likely that the Re-Os age is on the younger side of the 757 ± 6.8 Ma age, based on the suggested sediment accumulation rates.

Cawood et al. (2012) published models indicating what ages of zircon could be predicted to accumulate in a basin based on the tectonic setting. In their analysis of rift basins they determined that grains with ages within 150 My of the depositional age would reflect magmatic activity related to the rifting driving deposition. This increases the plausibility of a scenario in which the zircons cooled from melt and were deposited rapidly thereafter. This scenario could also explain why we do not see the ~775 grains in the stratigraphically higher Outlaw Trail and Moosehorn Lake formations of the UMG, as the ~775 Ma volcanic source was no longer available on the landscape. We hypothesize that further analysis of the Neoproterozoic zircons in the basal Jesse Ewing Canyon Fm will likely reveal a similar 775 Ma maximum depositional age for the true base of the UMG, also reflecting rift basin formation and regional volcanism at this time.

Volcanic source for Neoproterozoic zircons

The exact source of the ~775 Ma zircons identified in this study may be reduced to 3 known options, based on their timing of ~775 Ma and the proximity to

the ChUMP basins. Beyond these three sources the possibility remains that the ~775 Ma zircons originated during a currently unrecognized magmatic event.

The Gunbarrel magmatic event occurred along the margin of Laurentia at 780.3 ± 1.4 (Harlan et al., 2003), an age obtained from precise U-Pb dating of igneous baddeleyite. This event is recorded in the Hattah mafic intrusions, which are coarse grained tholeiitic subalkaline gabbro dikes and sheets that locally grade into more felsic compositions (Fraser, 1964). Its location on the western edge of Laurentia (where the CHUMP basins formed) and ~780 Ma timing make this event a likely source for the ~775 Ma zircons. Of the basins we studied, the UMG basin formed in the closest proximity to this magmatic event, and yet the UMG samples analyzed in this study are devoid of the 775 Ma population. The UMG zircons utilized in this study were taken from many meters above the base of the formation while the Chuar and Pahrump zircons were sampled a few meters above the base of their respective formations. If the three units are truly correlative as has been interpreted, we hypothesize that the ~775 Ma population will be present closer to the base of the UMG, in the basal Jesse Ewing Canyon Formation. Future CA-ID-TIMs analyses on the basal Jesse Ewing Canyon Fm. detrital zircons should be performed to clarify this discrepancy.

The Boucaut Volcanics in the Nackara Arc, South Australia, provide an alternative for the source of the ~775 Ma zircons. These rocks are a bimodal suite of amygdaloidal basalt and rhyolitic ignimbrite (Forbes, 1978). The rhyolites have provided U-Pb SHRIMP zircon ages of 777 ± 7 Ma (Preiss, 2000). The Australian

continents' potential location west of Laurentia during the rifting of Rodinia makes the location compelling as well (Li et al., 2008; 2013).

Another magmatic event produced the northern Daolinshan pluton, which was emplaced in present day South China. It resulted in the formation of a calc-alkaline granite-diabase complex that exhibits mainly medium to fine grained granitic textures. The granites provided a LA-ICP-MS age of 780 ± 6 Ma (Wang, 2010). The South China block is hypothesized to have bordered Laurentia to the northwest during the break up of Rodinia (Li et al., 2008; 2013).

Most ages from middle Neoproterozoic volcanic sources are reported with errors greater than 1%. To better understand the rifting of Rodinia and the source of middle Neoproterozoic detrital zircon populations, more high precision dating needs to be conducted on middle Neoproterozoic volcanic sources, as well as continued high precision dating of their detrital remains.

CONCLUSIONS

The significant zircon population with a mean age of 775.63 ± 0.27 Ma at the base of the Nankoweap Formation and the zircon population with a mean age of 775.44 ± 0.73 Ma at the base of the Horse Thief Springs formation provide refined maximum depositional ages for these units and highlight the parallels in timing of basin formation, paleogeography, and source area indicated by previous studies. The ~775 Ma age places new constraints on biotic and geochemical changes occurring during ChUMP time, from ~775 Ma to ~729 Ma, for a total maximum duration of 46 million years, changing the duration from previous estimates for the Chuar (Dehler et al., 2001; Dehler et al., 2017).

This study demonstrates the ability of careful CA-ID TIMS work following significant LA-ICP MS work to gain higher precision ages. In this case, the re-evaluation of zircons already identified as being Neoproterozoic via LA-ICP-MS analysis significantly refined the original ages. While it would be unreasonable to subject a complete sample of detrital material to CA-ID TIMS, utilizing zircons that have already been shown to fall within an age group significantly reduces the sample size, and provides a way to obtain more robust data from the same grains.

The data recovered from the Uinta Mountain Group zircons, though sparse, echo the results of previous work and provide further evidence to suggest a maximum depositional age of ~766 Ma for the lower-middle sections of the unit. This age is consistent with previously reported detrital zircon ages from the basal

UMG of being ~780 Ma. Future work may show that the basal UMG also has a maximum depositional age of ~775 Ma.

The uncertainty of the source area for the ~775 Ma grains illustrates the need for higher precision dating of igneous rocks of this age range. Without the ability to pinpoint the original source of the zircons in this study there is a limited amount of information we can extrapolate from the age alone. At the precision provided by CA-ID-TIMS, a difference of only a few million years between the ages from a possible source and those from the sedimentary record could disqualify that potential source as a possibility. These discrepancies could provide useful for future paleogeographic and plate tectonic reconstructions.

REFERENCES

Brehm, A., and Dehler, C., 2005, Re-evaluation of the Neoproterozoic Jesse Ewing Canyon Formation, Eastern Uinta Mountain Group, Northeastern Utah (abstract): Geological Society of America, Abstracts with Programs, v. 37, no. 7, p. 217.

Brehm, A., and Dehler, C., 2006, The new and improved Neoproterozoic Jesse Ewing Canyon Formation, basal Uinta Mountain Group, northeastern Utah and northwestern Colorado (abstract): Geological Society of America, Abstracts with Program, v. 38, no. 7, p. 494.

Brehm, Andrew M., 2007, Re-evaluation of the Jesse Ewing Canyon formation: Implications for Neoproterozoic Paleogeography and Tectonic Setting of Northeastern Utah [M.S. thesis]: Utah State University, 232 p.

Chumakov, N.M., 2009. The Baykonurian glaciohorizon of the Late Vendian. Stratigraphy and Global Correlation 17, 373–381.

Craddock, J.P., Schmitz, M.D., Crowley, J.L., Larocque J., Pankhurst R.J., Juda N., Konstantinou A., and Storey B. 2016. Precise U-Pb zircon ages and geochemistry of Jurassic granites, Ellsworth-Whitmore terrane, central Antarctica. Geological Society of America Bulletin. B31485-1.

Dalton, R.O., Jr., 1972, Stratigraphy of the Bass Formation (Late Precambrian, Grand Canyon, Arizona) [M.S. thesis]: Flagstaff, Northern Arizona University, 140 p.

Davydov, V.I., Crowley, J.L., Schmitz, M.D., Poletaev, V.I., 2010. High-precision U–Pb zircon age calibration of the global Carboniferous time scale and Milankovitch band cyclicity in the Donets Basin, eastern Ukraine. Geochemistry, Geophysics, Geosystems 1, Q0AA04.

De Grey, L.D., and Dehler, C.M., 2005, Stratigraphy and facies analysis of the eastern Uinta Mountain Group, Utah-Colorado border region, *in* Dehler, C.M., Pederson, J.L., Sprinkel, D.A., and Kowallis, B.J., eds., Uinta Mountain Geology: Utah Geological Association Publication 33, p. 31-47.

Dehler, C.M., Elrick, M.E., Karlstrom, K.E., Smith, G.A., Crossey, L.J., and Timmons, M.J., 2001, Neoproterozoic Chuar Group (~800–742 Ma), Grand Canyon: A record of cyclic marine deposition during global cooling and supercontinent rifting: Sedimentary Geology, v. 141–142, p. 465–499

Dehler, C.M., Elrick, M.E., Bloch, J.D., Karlstrom, K.E.,Crossey, L.J., and Des Marais, D., 2005, High resolution□13C stratigraphy of the Chuar Group (~770–742 Ma), Grand Canyon: Implications for mid-Neoproterozoic climate change: Geological Society of America Bulletin, v. 117, no. 1–2, p. 32–45

Dehler, C.M., Porter, S.M., De Grey, L.D., Sprinkel, D.A., and Brehm, A., 2007, The Neoproterozoic Uinta Mountain Group Revisited: A synthesis of recent work on the Red Pine Shale and related undivided clastic strata, Northeastern Utah, *in* Link, P.K., and Lewis, R.S., eds., Proterozoic Geology of western North America and Siberia: Society for Sedimentary Geology (SEPM) Special Publication 86, p. 151–166.

Dehler, C.M., Fanning, C.M., Link, P.K., Kingsbury, E.M., and Rybczynski, D., 2010, Maximum depositional age and provenance of the Uinta Mountain Group and Big Cottonwood Formation, northern Utah: Paleogeography of rifting western Laurentia: Geological Society of America Bulletin, v. 122, p. 1686–1699

Carol Dehler, George Gehrels, Susannah Porter, Matt Heizler, Karl Karlstrom, Grant Cox, Laura Crossey, Mike Timmons;, 2017, Synthesis of the 780–740 Ma Chuar, Uinta Mountain, and Pahrump (ChUMP) groups, western USA: Implications for Laurentia-wide cratonic marine basins. *GSA Bulletin* ; 129 (5-6): 607–624.

Dickin, A.P., 2005. *Radiogenic isotope geology*. Cambridge University Press. Print.

Ehlers, T.A., and Chan, M., 1999, Tidal sedimentology and estuarine deposition of the Proterozoic Big Cottonwood Formation, Utah: Journal of Sedimentary Research, v. 69, no. 6, p. 1169–1180

Elston, D.P., and Scott, G.R., 1976, Unconformity at the Cardenas-Nankoweap contact (Precambrian), Grand Canyon Supergroup, northern Arizona: Geological Society of America Bulletin, v. 87, p. 1763– 1772

Elston, D.P., 1979, Late Precambrian Sixtymile formation and orogeny at top of the Grand Canyon Supergroup, northern Arizona. (No. 1092). US Govt. Print. Off.,.

Feng, R., Machado, N. and Ludden, J., 1993. Lead geochronology of zircon by LaserProbe-Inductively coupled plasma mass spectrometry (LP ICPMS). *Geochimica et Cosmochimica Acta*, *57*(14), pp.3479-3486.

Forbes, B.G., 1978, The Boucaut Volcanics. South Australian Geol. Survey Quart. Geol. Notes 65, 6–10.

Ford, T.D., Breed, W.J., 1973, Late Precambrian Chuar Group, Grand Canyon, Arizona. Geol. Soc. Am. Bull. 84, 1243-1260.

Fraser, J.A., 1964, Geological notes on the Northeastern District of Mackenzie, Northwest Territories: Geological Survey of Canada Paper 63-40, 20 p.

Gebel, D.C., 1978, Stratigraphy of the Nankoweap Formation, eastern Grand Canyon, Arizona [M.S. thesis]: Flagstaff, Northern Arizona University, 129 p.

Gehrels, G.E., 2012, Detrital zircon U-Pb geochronology: Current methods and new opportunities, *in* Busby, C., and Azor, A., eds., Tectonics of Sedimentary Basins: Recent Advances: Hoboken, New Jersey, Blackwell Publishing Ltd., p. 47–62.

Hansen, W.R., 1965, Geology of the Flaming Gorge Area, Utah-Colorado-Wyoming: U.S. Geological Survey Professional Paper 490, 196 p.

Hendricks, J.D., 1972, Younger Precambrian basaltic rocks of the Grand Canyon, Arizona [M.S. thesis]: Flagstaff, Northern Arizona University, 122 p.

Hendricks, J.D., and Stevenson, G.M., 1990, Grand Canyon Supergroup: Unkar Group, *in* Beus, S.S., and Morales, M., eds., Grand Canyon geology: Oxford, Oxford University Press, and Flagstaff, Museum of Northern Arizona Press, p. 29–47.

Hill, A.C., Cotter, K.L., and Grey, K., 2000, Mid-Neoproterozoic biostratigraphy and isotope stratigraphy in Australia: Precambrian Research, v. 100, p. 281–298

Hinton, R.W., 1995. Ion microprobe analysis in geology. In *Microprobe techniques in the Earth Sciences.* pp. 235-289. Springer US.

Hoffman, P.F., Kaufman, A.K., Halverson, G.P., and Schrag, D.P., 1998, A Neoproterozoic Snowball: Earth Science, v. 281, p. 1342–1346.

Hoffman, P. F., Halverson, G. P., Domack, E. W., Maloof, A. C., Swanson-Hysell, N. L. & Cox, G. M. 2012, Cryogenian glaciations on the southern tropical paleomargin of Laurentia (NE Svalbard and East Greenland), and a primary origin for the upper Russoya (Islay) carbon isotope excursion. Precambrian Research, 206, 137–158.

Horodyski, R.J., 1993, Paleontology of Proterozoic shales and mudstones: Examples from the Belt Supergroup, Chuar Group, and Pahrump Group, western U.S.A: Precambrian Research, v. 61, p. 241–278

Horodyski, R. 1987, A new occurrence of the vase-shaped fossil Melanocyrillium and new data on this relatively complex late Precambrian fossil. Geological Society of America, Boulder, CO, Melanocyrillium.

Kingsbury-Stewart, E.M., Osterhout, S.L., Link, P.K., and Dehler, C.M., 2013, Sequence stratigraphy and formalization of the Middle Uinta Mountain Group (Neoproterozoic), central Uinta Mountains, Utah: A closer look at the western Laurentian Seaway at ca. 750Ma: Precambrian Research, v. 236, p. 65-84.

Kozakov, I.K., Bibikova, E.V., Neymark, L.A., Kirnozova, T.I., 1993, The Baydaric block. In: Rudnik, B.A., Sokolov, Y.M., Filatova, L.I. (Eds.), Early Precambrian of the Central Asian Fold Belt. Nauka, St. Petersburg, pp. 118–137.

Labotka, T. C., Albee, A. L., Lanphere, M. A., and McDowell, S. C., 1980, Stratigraphy, structure and metamorphism in the central Panamint Mountains (Telescope Peak quadrangle), Death Valley area, California: Geological Society of America Bulletin, v. 91, part II, p. 843–933.

Levashova, N.M., Meert, J.G., Gibsher, A.S., Grice, W.C., Bazenhov, M.L., 2011, The origin of microcontinents in the Central Asian Orogenic Belt: Constraints from paleomagnetism and geochronology. Precambrian Research 185, 37–54.

Licari, G. R. 1978, Biogeology of late Pre-Phanerozoic Beck Spring Dolomite of eastern California. Journal of Paleontology, 52, 767–792.

Link, P.K., Christie-Blick, N., Stewart, J.H., Miller, J.M.G., Devlin, W.J., Levy, M., 1993, Late Proterozoic strata of the United States Cordillera. In: Link, P.K. (Ed.), Middle and Late Proterozoic stratified rocks of the western U.S. Cordillera, Colorado Plateau, and Basin and Range Province. In: Reed Jr., J.C. (Ed.), Precambrian: Conterminous U.S., vol. C-2, pp. 536–558 (Chapter 6).

Lucchitta, I., and Hendricks, J.D., 1983, Characteristics, depositional environment, and tectonic interpretations of the Proterozoic Cardenas Lavas, eastern Grand Canyon, Arizona: Geology, v. 11, p. 177–181

Macdonald, F. A., Prave, A. R., et al. 2013, The Laurentian record of Neoproterozoic glaciation, tectonism, and eukaryotic evolution in Death Valley, California. Geological Society of America Bulletin, 125, 1203–1223

Mahon R.C., (Idaho State University Thesis) 2012, Detrital zircon provenance, geochronology and revised stratigraphy of the Mesoproterozoic and Neoproterozoic Pahrump (Super)Group, Death Valley region, California AND Geology of the Saddle Peak Hills 7.5 quadrangle, San Bernardino County, California, 194pp.

Mahon, R.C., Link, P.K., 2011, Seismites and evidence for syn-depositional extensional tectonism from the Beck Spring Dolomite (Pahrump Group), southeastern Death Valley, California. Geol. Soc. Am. Abs. Prog. 43 (5), p280.

Mahon, R.C., Dehler, C.M., Link, P.K., Karlstrom, K.E., Gehrels, G.E., 2014, Geochronologic and stratigraphic constraints on the Mesoproterozoic and Neoproterozoic Pahrump Group, Death Valley, California: a record of the assembly and breakup of Rodinia. Geol. Soc. Am. Bull. 126 (5–6), p. 619–638

Mattinson, J. M. 2005, Zircon U–Pb chemical abrasion ("CA-TIMS") method: combined annealing and multi-step partial dissolution analysis for improved precision and accuracy of zircon ages. *Chemical Geology*, *220*(1), 47-66.

Meert, J. G., Gibsher, A. S., Levashova, N. M., Grice, W. C., Kamenov, G. D., & Ryabinin, A. B. 2011, Glaciation and~ 770Ma Ediacara (?) Fossils from the Lesser Karatau Microcontinent, Kazakhstan. *Gondwana Research*, *19*(4), 867-880.

Miller, J. M. G., 1985, Glacial and syntectonic sedimentation: The Upper Proterozoic Kingston Peak Formation, southern Panamint Range, eastern California: Geological Society of America Bulletin, v. 96, p. 1537–1553.

Mueller, P.A., and Frost, C.D., 2006, The Wyoming Craton: A distinctive Archean craton in Laurentian North America: Canadian Journal of Earth Sciences, v. 43, p. 1391–1397

Nagy, R., Porter, S., Dehler, C.M., and Shen, Y., 2009, Biotic turnover driven by eutrophication before low latitude glaciation: Nature Geoscience: Letters, v. 2, p. 415–418.

Nelson, S.T., Hart, G.L. and Frost, C.D., 2011. A reassessment of Mojavia and a new Cheyenne Belt alignment in the eastern Great Basin. *Geosphere*, *7*(2), pp.513-527.

Porter, Susannah M., 2016, Tiny vampires in ancient seas: evidence for predation via perforation in fossils from the 780–740 million-year-old Chuar Group, Grand Canyon, USA. *Proc. R. Soc. B*. Vol. 283. No. 1831, p.20160221.

Porter, S.M. & Knoll, A. H., 2000, Testate amoebae in the Neoproterozoic Era: evidence from vase-shaped microfossils in the Chuar Group, Grand Canyon. Paleobiology, 26, 360–385.

Prave, A.R., 1999, Two diamictites, two cap carbonates, two delta C-13 excursions, two rifts: the Neoproterozoic Kingston Peak Formation, Death Valley, California. Geology 27, 339–342.

Reed, V.S., 1976, Stratigraphy and depositional environment of the upper Precambrian Hakatai Shale, Grand Canyon, Arizona [M.S. thesis]: Flagstaff, Northern Arizona University, 163 p.

Roberts, M.T., 1976, Stratigraphy and depositional environments of the Crystal Spring Formation, southern Death Valley region, California. California Division of Mines and Geology Special Report 106, pp. 35–44.

Roberts, M.T., 1982, Depositional environments and tectonic setting of the Crystal Spring Formation, Death Valley, California. In: Cooper, J.D., Troxel, B.W., Wright, L.A. (Eds.), Geology of selected areas in the San Bernardino Mountains, Western Mojave Desert, and southern Great Basin, California: Volume and guidebook for field trip no. 9, 78th Anniversary Meeting of Cordilleran Section, Geological Society of America. Death Valley Publishing Company, Shoshone, CA, pp. 165–170.

Rooney, A.D., Austermann, J., Smith, E.F., Li, Y., Selby, D., Dehler, C.M., Schmitz, M.D., Karlstrom, K.E. and Macdonald, F.A., 2017. Coupled Re-Os and U-Pb geochronology of the Tonian Chuar Group, Grand Canyon. Geological Society of America Bulletin.

Rybczynski, D., 2009, Correlation, paleogeography, and provenance of the eastern Uinta Mountain Group, Goslin Mountain area, Daggett County, northeastern Utah [M.S. thesis]: Logan, Utah State University, 224 p.

Schmitz, M. D., & Schoene, B. 2007, Derivation of isotope ratios, errors, and error correlations for U-Pb geochronology using 205Pb-235U-(233U)-spiked isotope dilution thermal ionization mass spectrometric data. Geochemistry, Geophysics, Geosystems, 8(8).

Schmitz, M. D., & Davydov, V. I. 2012, Quantitative radiometric and biostratigraphic calibration of the Pennsylvanian–Early Permian (Cisuralian) time scale and pan-Euramerican chronostratigraphic correlation. Geological Society of America Bulletin, 124(3-4), 549-577.

Sears, J.W., 1990, Geologic structure of the Grand Canyon Supergroup. In: Beus, S.S., Morales, M. (Eds.), Grand Canyon Geology. Oxford University Press, New York, pp. 71–82.

Smith, E. F., MacDonald, F. A., Crowley, J. L., Hodgin, E. B., Schrag, D. P. 2015, Tectonostratigraphic evolution of the c. 780–730 Ma Beck Spring Dolomite: Basin Formation in the core of Rodinia. *Geological Society, London, Special Publications*, *424*(1), pp.213-239.

Sprinkel, D. A., & Waanders, G. 2005, Stratigraphy, organic microfossils, and thermal maturation of the Neoproterozoic Uinta Mountain Group in the eastern Uinta Mountains, Northeastern Utah. 63-742.

Sprinkel, D., 2006, Interim Geological Map of the Dutch John 30 X 60 Quadrangle, Daggett and Uintah Counties, Utah, Moffat County, Colorado and Sweetwater County Wyoming, USGS Open File Report 491DM.

Strauss, J.V., Rooney, A.D., MacDonald, F.A., Brandon, A.D., and Knoll, A.H., 2014, 740 Ma vase-shaped microfossils from Yukon, Canada: Implications for Neoproterozoic chronology and biostratigraphy: Geology, v. 42, p. 659– 662

Timmons, M.J., Karlstrom, K.E., Dehler, C.M., Geissman, J.W., and Heizler, M.T., 2001, Proterozoic multistage (~1.1 and ~0.8 Ga) extension in the Grand Canyon Supergroup and establishment of northwest and north-south tectonic grains in the southwestern United States: Geological Society of America Bulletin, v. 113, p. 163–181

Timmons , J.M., Karlstrom, K.E., Heizler, M.T., Bowring, S.A., Gehrels, G.E., Crossey, L.J., 2005, Tectonic inferences from the ca.1255-1100 Ma Unkar Group and Nankoweap Formation, Grand Canyon: Intracratonic deformation and basin formation during protracted Grenville orogenesis: GSA Bulletin, v. 117, no. 11/12, p. 1573-1595.

Troxel, B.W., 1967, Sedimentary rocks of late Precambrian and Cambrian age in the southern Salt Spring Hills, southeastern Death Valley, California. Short Contributions to California Geology, California Division of Mines and Geology, Special Report 92, pp. 33–42.

Tucker, M. E., 1983, Diagenesis, geochemistry, and origin of a Precambrian dolomite: the Beck Spring Dolomite of eastern California. *Journal of Sedimentary Research*, *53*(4).

Van Gundy, C.E., 1951, Nankoweap Group of the Grand Canyon Algonkian of Arizona: Geological Society of America Bulletin, v. 62, p. 953–959.

Vidal, G., and Ford, T.D., 1985, Microbiotas from the Late Proterozoic Chuar Group (northern Arizona) and Uinta Mountain Group (Utah) and their chronostratigraphic implications. Precambrian Research, vol. 28, pp. 349-389.

Wallace, C.A., 1972, A basin analysis of the upper Precambrian Uinta Mountain Group, Utah [Ph.D. thesis]: Santa Barbara, University of California, p. 412.

Wallace and Crittenden, M.D., 1969, The Stratigraphy, depositional environment and correlation of the Precambrian Uinta Mountain Group, western Uinta Mountains, Utah, *in* Lindsey, J.B., editor, Geologic Guidebook of the Uinta Mountains: Intermountain Association of G4eologists and Utah Geological Society 16th Annual Field Conference, p. 127-142.

Wang, Q., Wyman, D.A., Li, Z.X., Bao, Z.W., Zhao, Z.H., Wang, Y.X., Jian, P., Yang, Y.H. and Chen, L.L., 2010. Petrology, geochronology and geochemistry of ca. 780 Ma A-type granites in South China: petrogenesis and implications for crustal growth

during the breakup of the supercontinent Rodinia. *Precambrian Research*, *178*(1-4), pp.185-208.

Wasserburg, G.J., Wetherill, G.W., Wright, L.A., 1959, Ages in the Precambrian terrane of Death Valley, California. J. Geol. 67, 702–708.

Weil, A.B, Geissman, J., Heizler, M., Van der Voo, R.A., 2003, Paleomagnetic investigation of Middle Proterozoic mafic intrusions and Upper Proterozoic redbeds from the Lower Grand Canyon Supergroup, Arizona. Tectonophysics 375, 199–220.

Weil, A.B., Geissman, J., Van der Voo, R., 2004, Paleomagnetism of the Neoproterozoic Chuar Group, Grand Canyon Supergroup, Arizona: implications for Laurentia's Neoproterozoic APWP and Rodinia break-up. Precambrian Res. 129, 71–92.

Weil, A., Geissman, J., and Ashby, J.M., 2006, A new paleomagnetic pole for the Neoproterozoic Uinta Mountain supergroup, Rocky Mountain States, U.S.A.: Precambrian Research, v. 147, p. 234–259

Wright, L. A., Troxel, B.W., Williams, E. G., Roberts, M. T., and Diehl, P. E., 1976, Precambrian sedimentary environments of the Death Valley region, eastern California: California Division of Mines and Geology Special Report 106, p. 7–15.

Zempolich, W.G., 1989, Meteoric stabilization and preservation of limestone within the Late Proterozoic Beck Spring Dolomite of eastern California. In: Cooper, J.D. (Ed.), Volume and Guidebook: Cavalcade of Carbonates. The Pacific Section SEPM, pp. 61–75.

APPENDICES

Appendix A: Sample Locations

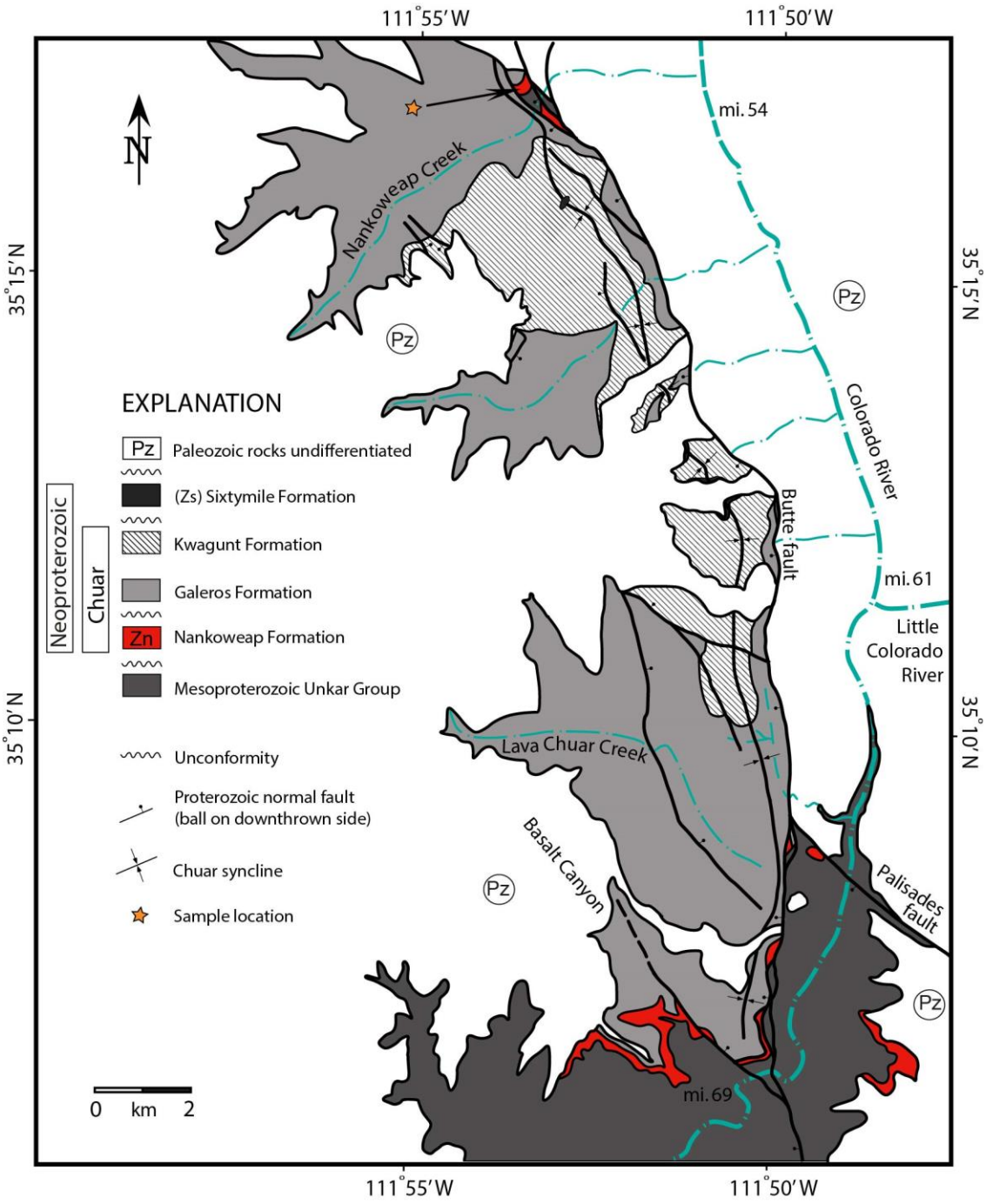

Geologic map of the Chuar Group, Grand Canyon, Arizona, showing the location of the sample site. Modified from Timmons et al., 2001, and Dehler et al., 2017.

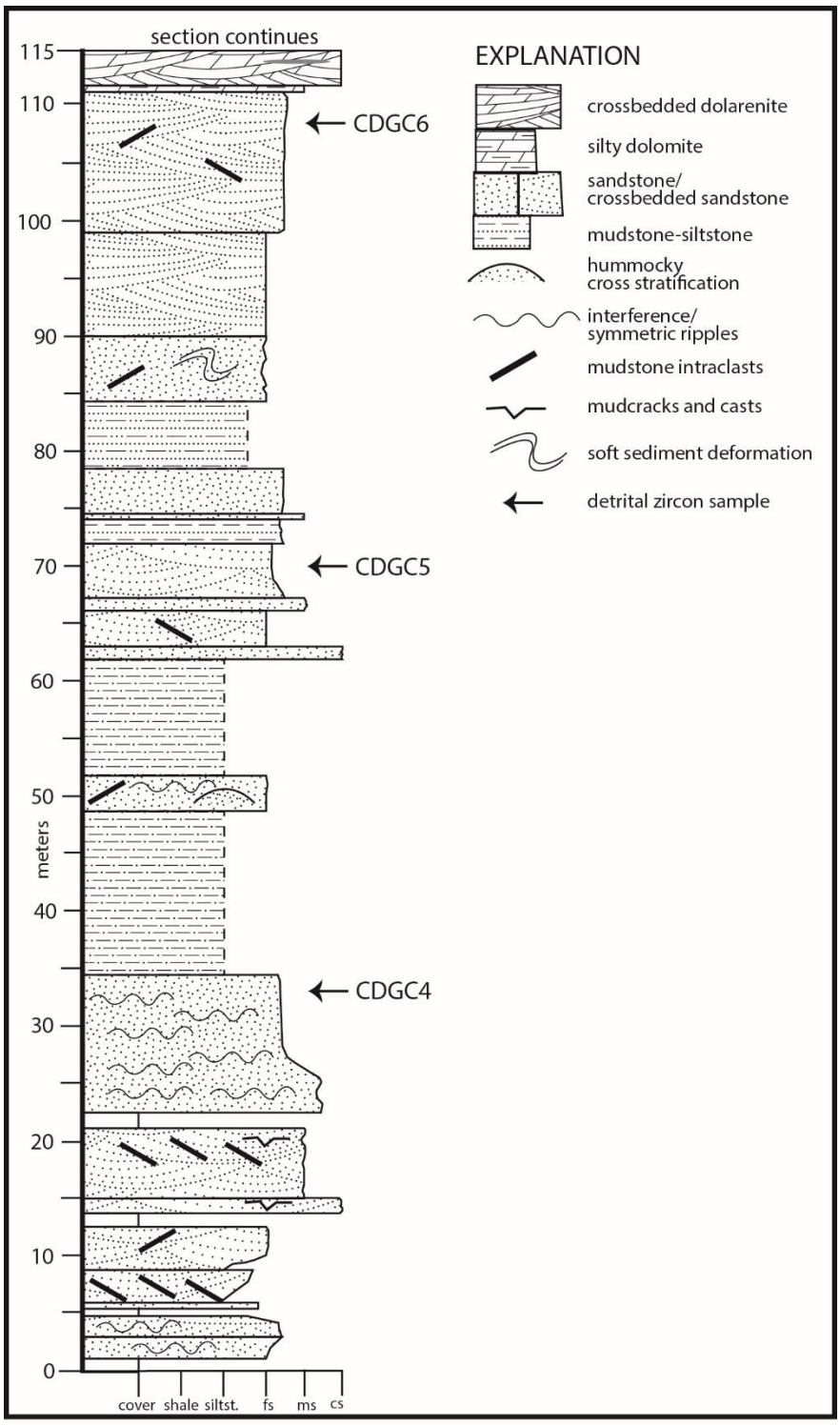

Stratigraphic column of the Nankoweap Formation, Chuar Group, showing sample locations. Modified from Dehler et al., 2017.

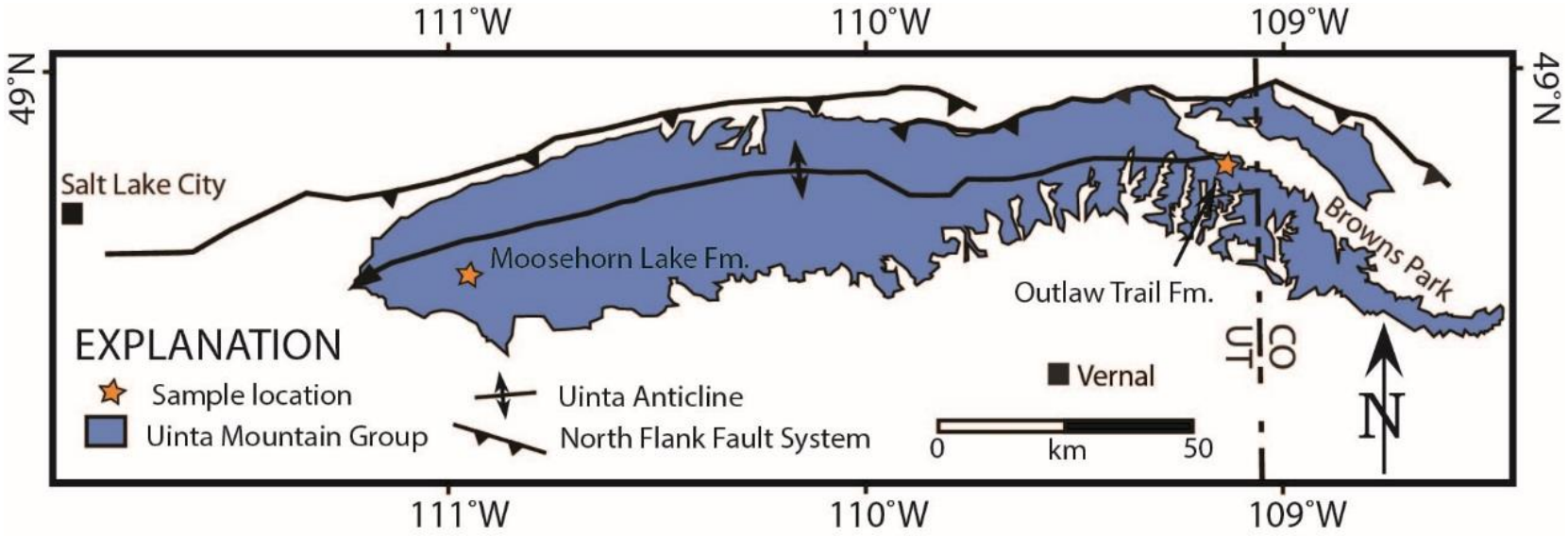

Geologic map of the Uinta Mountain Group, Northeastern Utah, showing the location of the sample sites. Modified from Dehler et al., 2010

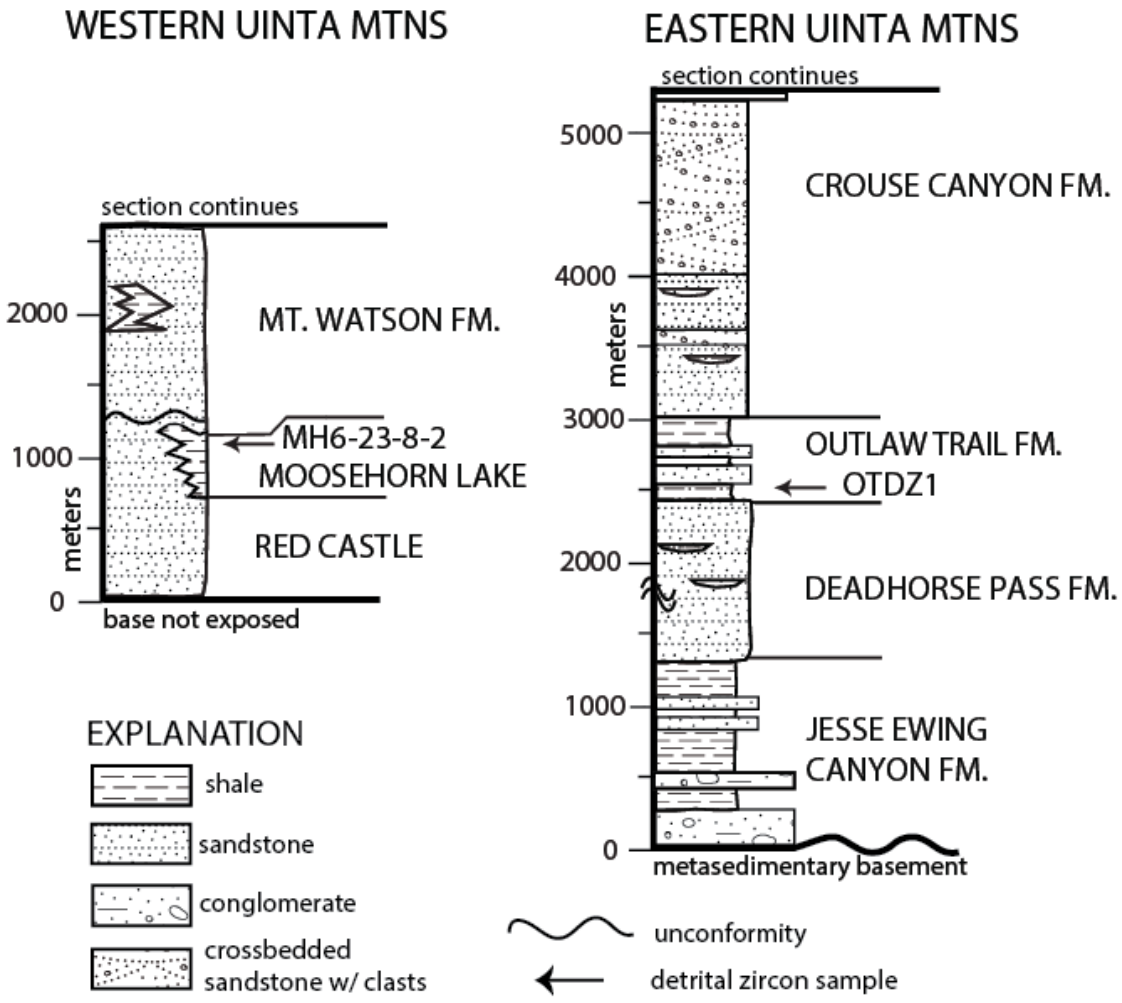

Stratigraphic column of the western and eastern sections of the lower Uinta Mountain Group with sample positions marked. Modified from Dehler et al., 2010.

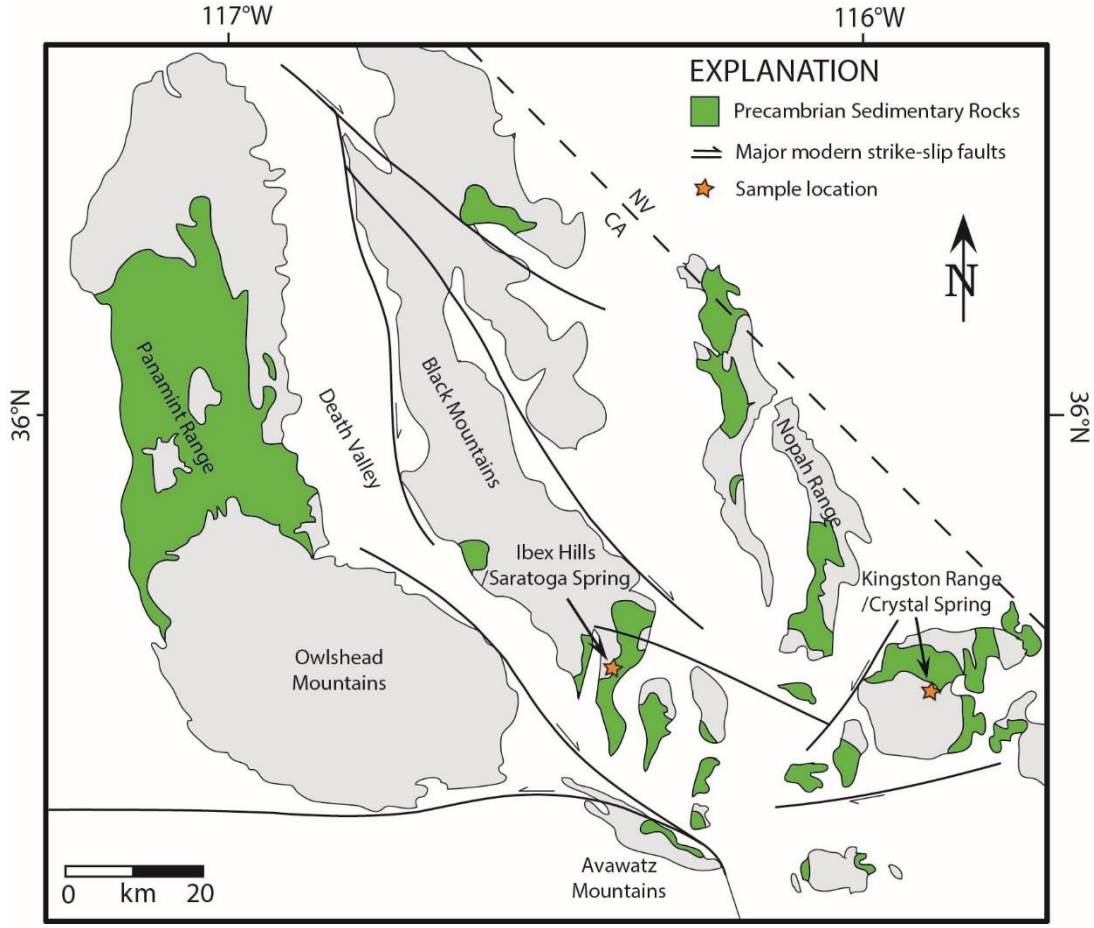

Geologic map of the Pahrump Group, Death Valley, California, showing the location of the sample sites. Modified from Mahon et al., 2014.

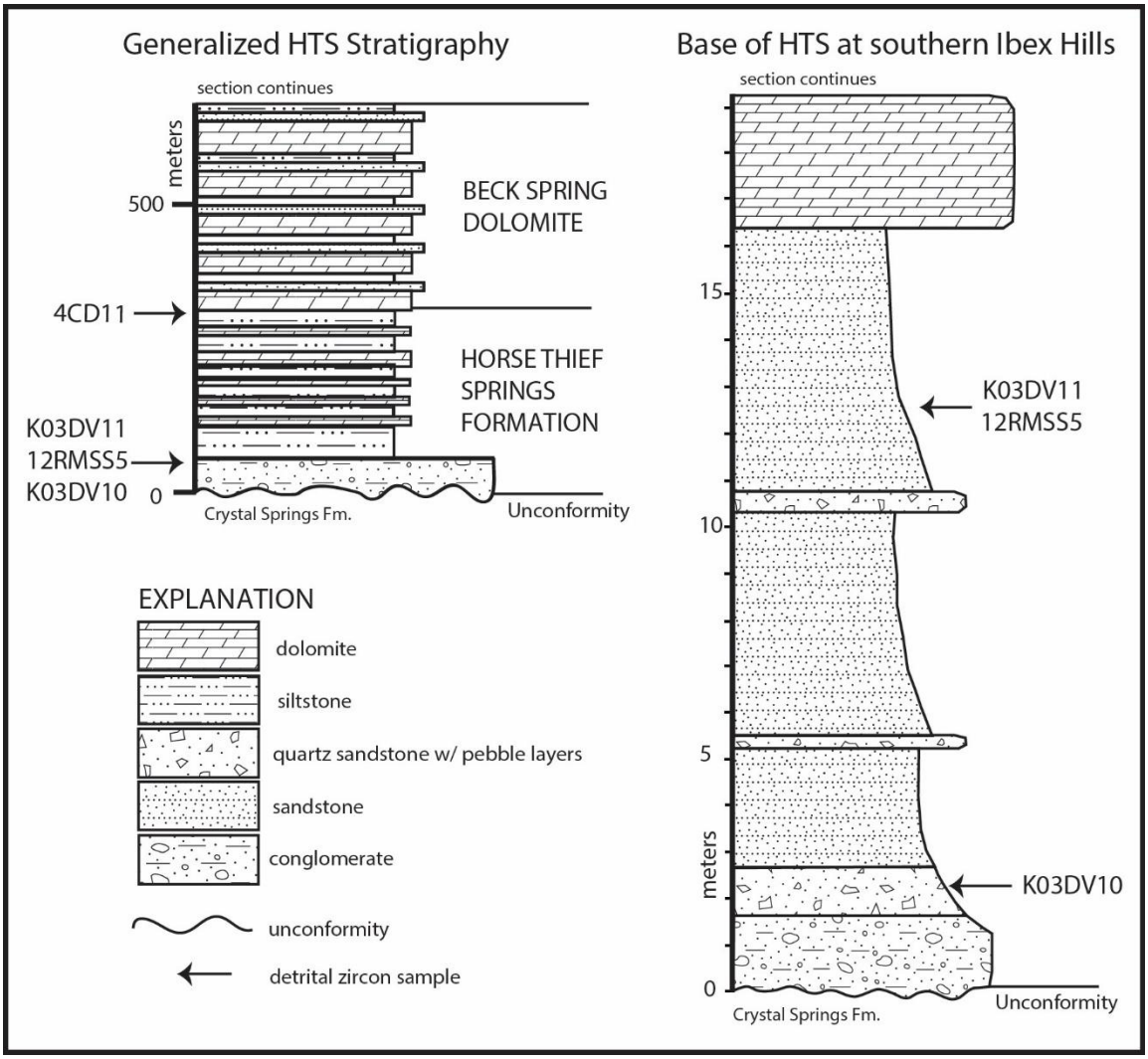

Generalized stratigraphic column of the Horse Thief Springs Formation, Pahrump Group showing sample positions, at left. At right is a detailed column of the lowermost portion of the Horse Thief Springs Formation from the Ibex Hills Saratoga Springs locality. Modified from Mahon et al. 2014.

Appendix B: Young Zircons

Description of ~775 Ma Chuar Grains

CDGC4-z1 provided an isotopic age of 775.53 ± 1.44 Ma. It is elongate and sub-rounded and ~59 microns x 183 microns. It has multiple generations of rim.

CDGC4-z3 provided an isotopic age of 776.04 ± 0.98 Ma. It is barely elongate, sub-rounded to rounded, and ~72 microns x 125 microns. It has hourglass zoning with a rim.

CDGC4-z4 provided an isotopic age of 775.42 ± 1.03 Ma. It is a barely elongate, well rounded euhedral grain, measuring ~40 microns x 70 microns. It exhibits some zoning.

CDGC4-z5 provided an isotopic age of 775.74 ± 1.22 Ma. It is a rounded euhedral grain, measuring ~45 microns x 75 microns. It exhibits some zoning.

CDGC4-z6 provided an isotopic age of 776.51 ± 1.34 Ma. It is an elongate, angular to sub-angular grain, measuring ~33 microns x 100 microns. It exhibits vague hourglass zoning.

CDGC4-z7 provided an isotopic age of 774.99 ± 1.54 Ma. It is a sub-rounded to rounded euhedral grain, measuring ~33 microns x 70 microns. Some zoning is present.

CDGC4-z8 provided an isotopic age of 775.21 ± 1.64 Ma. It is an elongate sub-rounded grain measuring ~26 microns x 85 microns. Some zoning is present.

CDGC4-z9 provided an isotopic age of 775.74 ± 1.22 Ma. It is broken and sub-angular, and measures ~36 microns x 50 microns. No zoning is visible.

CDGC4-z11 provided an isotopic age of 775.33 ± 0.89 Ma. It is an elongate, rounded euhedral crystal, measuring ~41 microns x 90 microns. Some zoning is present.

CDGC4-z12 provided an isotopic age of 775.36 ± 2.13 Ma. It is a broken sub-angular to sub-rounded grain, measuring ~37 microns x 45 microns. Some zoning is present.

CDGC4-z13 provided an isotopic age of 775.79 ± 0.81 Ma. It is an elongate sub-angular grain, measuring ~36 microns x 91 microns. No zoning is visible.

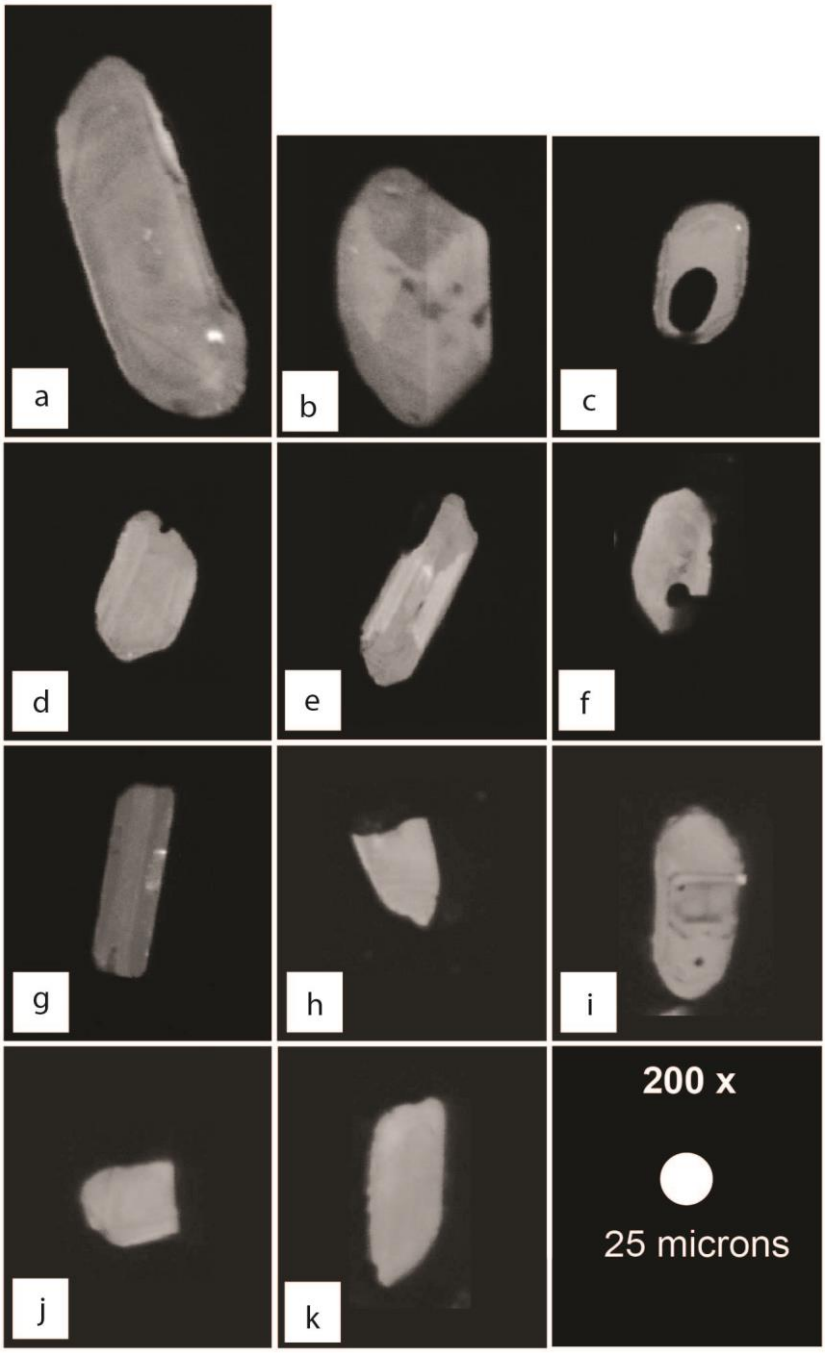

Images of CDGC4 zircons with young ages in TIMS. a) z1; b) z3; c) z4; d) z5; e) z6; f) z7; g) z8; h) z9; i) z11; j: z12; k) z13

Description of ~775 Ma Pahrump Grains

12RMSS5-z1 provided an isotopic age of 775.49 ± 1.25 Ma. It is a highly elongate sub-rounded to rounded grain, measuring ~40 microns x 120 microns. Exhibits hourglass zoning, with the crux far toward the wider end.

12RMSS5-z4 provided an isotopic age of 775.34 ± 0.91 Ma. It is a rounded grain, measuring ~40 microns x 61 microns. Exhibits some zoning.

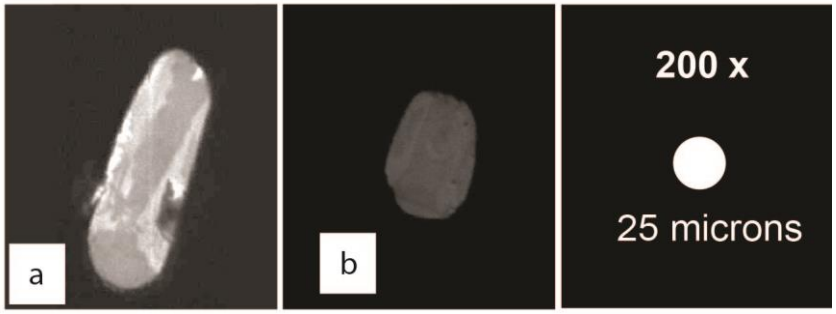

Images of RM12SS5 zircons with young ages in TIMS. a) z1; b) z4

Appendix C: Compositional parameters for isotopic analyses

Chuar Sample (a)	Th/U (b)	$^{206}Pb^*$ x10^{-13} mol (c)	mol % $^{206}Pb^*$ (c)	Pb^*/Pb_c (c)	Pb_c (pg) (c)	$^{206}Pb/^{204}Pb$ (d)
CDGC4-z1	0.873	0.1818	95.44%	7	0.72	392
CDGC4-z3	1.025	0.2165	97.65%	14	0.43	769
CDGC4-z4	0.804	0.3224	98.41%	20	0.43	1137
CDGC4-z5	0.960	0.1685	97.55%	13	0.35	736
CDGC4-z6	1.001	0.1690	94.08%	5	0.89	300
CDGC4-z7	0.988	0.1471	95.92%	8	0.52	442
CDGC4-z8	0.962	0.1777	97.84%	15	0.33	835
CDGC4-z9	1.266	0.3507	98.56%	25	0.42	1256
CDGC4-z10	0.922	0.3037	97.81%	15	0.56	822
CDGC4-z11	1.325	0.3058	95.44%	8	1.23	388
CDGC4-z12	0.931	0.1439	97.05%	11	0.36	611
CDGC4-z13	1.001	0.3098	99.07%	37	0.24	1948
CDGC5-z2	0.808	0.8636	99.60%	81	0.29	4514
CDGC5-z3	0.323	0.4886	99.46%	55	0.22	3349
CDGC5-z4	0.434	0.0635	95.69%	7	0.24	418
CDGC5-z6	1.067	0.2472	98.86%	30	0.24	1579
CDGC5-z7	0.035	0.5798	99.51%	54	0.24	3654
CDGC5-z9	0.755	0.2147	98.26%	18	0.32	1037
CDGC6-z1	1.818	0.9311	99.43%	70	0.45	3144
CDGC6-z2	0.285	4.5486	97.61%	12	9.26	753
NAN1-z1	1.145	0.2796	97.40%	13	0.62	695

UMG Sample (a)	Th/U (b)	$^{206}Pb^*$ x10^{-13} mol (c)	mol % $^{206}Pb^*$ (c)	Pb^*/Pb_c (c)	Pb_c (pg) (c)	$^{206}Pb/^{204}Pb$ (d)
MH6-23-6-z4	0.695	0.0886	95.91%	7.5	0.31	442
OTDZ-1-z1	0.650	0.7911	99.62%	83	0.25	4777
OTDZ-1-z2	0.255	2.0468	99.74%	108	0.45	6840
OTDZ-1-z3	0.461	0.5899	99.28%	41	0.35	2511

Pahrump Sample (a)	Th/U (b)	$^{206}Pb^*$ x10^{-13} mol (c)	mol % $^{206}Pb^*$ (c)	Pb^*/Pb_c (c)	Pb_c (pg) (c)	$^{206}Pb/^{204}Pb$ (d)
12RM-SS5-z1	1.008	0.3473	94.51%	5.8	1.70	321
12RM-SS5-z2	0.538	6.0064	99.68%	94	1.63	5486
12RM-SS5-z3	1.155	0.7013	95.79%	7.9	2.59	418
12RM-SS5-z4	0.908	0.2534	96.84%	10	0.69	566
12RM-SS5-z5	1.020	0.0678	89.16%	2.8	0.69	165
12RM-SS5-z6	0.402	1.8844	99.02%	30	1.57	1797
12RM-SS5-z7	0.176	0.5176	99.51%	57	0.21	3719
12RM-SS5-z8	0.478	0.4255	99.37%	48	0.23	2846
4CD-11-z1	0.666	0.1312	96.35%	8.4	0.41	495
4CD-11-z2	0.573	0.1501	94.34%	5.2	0.75	315
4CD-11-z3	0.532	0.1339	95.84%	7.1	0.48	433
4CD-11-z4	0.577	0.1649	97.80%	14	0.31	820

(a) z1, z2 etc. are labels for single zircon grains or fragments annealed and chemically abraded after Mattinson (2005).
(b) Model Th/U ratio iteratively calculated from the radiogenic 208Pb/206Pb ratio and 206Pb/238U age.
(c) Pb* and Pbc represent radiogenic and common Pb, respectively; mol % $^{206}Pb^*$ with respect to radiogenic, blank and initial common Pb.

(d) Measured ratio corrected for spike and fractionation only. Fractionation estimated at 0.20 +/- 0.03 %/a.m.u. for Daly analyses, based on analysis of NBS-981 and NBS-982.

Appendix D: Radiogenic Isotope Ratios

Chuar								
Sample	$^{208}Pb/^{206}Pb$	$^{207}Pb/^{206}Pb$	% err	$^{207}Pb/^{235}U$	% err	$^{206}Pb/^{238}U$	% err	corr. coef.
(a)	(e)	(e)	(f)	(e)	(f)	(e)	(f)	
CDGC4-z1	0.269	0.064734	0.693	1.141047	0.774	0.127841	0.197	0.514
CDGC4-z3	0.316	0.065081	0.443	1.147959	0.503	0.127930	0.134	0.556
CDGC4-z4	0.248	0.064884	0.287	1.143496	0.352	0.127820	0.140	0.621
CDGC4-z5	0.296	0.064896	0.452	1.144227	0.523	0.127877	0.167	0.554
CDGC4-z6	0.308	0.065107	0.683	1.149152	0.762	0.128012	0.183	0.527
CDGC4-z7	0.305	0.064889	0.724	1.142933	0.808	0.127746	0.211	0.508
CDGC4-z8	0.296	0.064681	0.437	1.139598	0.529	0.127784	0.224	0.585
CDGC4-z9	0.390	0.065063	0.279	1.147192	0.330	0.127879	0.104	0.606
CDGC4-z10	0.284	0.065260	0.373	1.154776	0.439	0.128335	0.145	0.581
CDGC4-z11	0.408	0.065152	0.397	1.148096	0.457	0.127806	0.122	0.595
CDGC4-z12	0.287	0.064841	0.636	1.142656	0.746	0.127811	0.292	0.545
CDGC4-z13	0.309	0.064994	0.287	1.146035	0.343	0.127886	0.110	0.625
CDGC5-z2	0.249	0.064964	0.141	1.136583	0.199	0.126890	0.066	0.915
CDGC5-z3	0.094	0.113942	0.083	5.256811	0.195	0.334608	0.144	0.922
CDGC5-z4	0.132	0.074561	0.973	1.846618	1.156	0.179624	0.501	0.552
CDGC5-z6	0.329	0.064968	0.245	1.145688	0.305	0.127898	0.114	0.661
CDGC5-z7	0.011	0.075656	0.132	1.896389	0.188	0.181796	0.089	0.770
CDGC5-z9	0.233	0.064801	0.383	1.142125	0.445	0.127830	0.132	0.590
CDGC6-z1	0.560	0.065847	0.127	1.200663	0.178	0.132246	0.071	0.815
CDGC6-z2	0.087	0.076348	0.134	1.918830	0.188	0.182279	0.074	0.823
NAN1-z1	0.353	0.064939	0.404	1.144229	0.464	0.127792	0.112	0.628

UMG								
Sample	$^{208}Pb/^{206}Pb$	$^{207}Pb/^{206}Pb$	% err	$^{207}Pb/^{235}U$	% err	$^{206}Pb/^{238}U$	% err	corr. coef.
(a)	(e)	(e)	(f)	(e)	(f)	(e)	(f)	
MH6-23-6-z4	0.214	0.064873	1.056	1.129960	1.167	0.126327	0.320	0.470
OTDZ-1-z1	0.201	0.064859	0.113	1.128071	0.167	0.126143	0.077	0.821
OTDZ-1-z2	0.078	0.069496	0.080	1.423423	0.140	0.148551	0.070	0.926
OTDZ-1-z3	0.143	0.059736	0.199	0.792518	0.253	0.096222	0.104	0.668

Pahrump Sample (a)	$^{208}Pb/^{206}Pb$ (e)	$^{207}Pb/^{206}Pb$ (e)	% err (f)	$^{207}Pb/^{235}U$ (e)	% err (f)	$^{206}Pb/^{238}U$ (e)	% err (f)	corr. coef.
12RM-SS5-z1	0.311	0.064960	0.449	1.144958	0.523	0.127833	0.171	0.565
12RM-SS5-z2	0.166	0.066054	0.071	1.203040	0.132	0.132092	0.065	0.965
12RM-SS5-z3	0.353	0.069657	0.257	1.466406	0.353	0.152682	0.193	0.703
12RM-SS5-z4	0.280	0.065095	0.418	1.147098	0.478	0.127807	0.125	0.577
12RM-SS5-z5	0.314	0.064074	2.464	1.131383	2.632	0.128064	0.528	0.409
12RM-SS5-z6	0.122	0.073433	0.110	1.733378	0.169	0.171200	0.077	0.856
12RM-SS5-z7	0.054	0.072157	0.111	1.501894	0.221	0.150959	0.158	0.880
12RM-SS5-z8	0.145	0.074890	0.184	1.857153	0.296	0.179856	0.180	0.808
4CD-11-z1	0.199	0.084404	0.676	2.603815	0.811	0.223741	0.338	0.575
4CD-11-z2	0.170	0.090069	0.581	3.078952	0.757	0.247928	0.404	0.652
4CD-11-z3	0.159	0.084607	0.687	2.622180	0.812	0.224779	0.329	0.552
4CD-11-z4	0.178	0.068138	0.459	1.254703	0.693	0.133551	0.475	0.751

(a) z1, z2 etc. are labels for single zircon grains or fragments annealed and chemically abraded after Mattinson (2005).
(e) Corrected for fractionation, spike, and common Pb; up to 0.5 pg of common Pb was assumed to be procedural blank: 206Pb/204Pb = 18.042 ± 0.61%; 207Pb/204Pb = 15.537 ± 0.52%; 208Pb/204Pb = 37.686 ± 0.63% (all uncertainties 1-sigma). Excess over blank was assigned to initial common Pb, using the Stacey and Kramers (1975) two-stage Pb isotope evolution model at the nominal sample age.
(f) Errors are 2-sigma, propagated using the algorithms of Schmitz and Schoene (2007).